INTRODUCTION TO QUANTUM INFORMATION AND COMPUTATION FOR CHEMISTRY

SABRE KAIS

Department of Chemistry and Physics, Purdue University, 560 Oval Drive, West Lafayette, IN 47907, USA; Qatar Environment & Energy Research Institute (QEERI), Doha, Qatar; Santa Fe Institute, Santa Fe, NM 87501, USA

Advances in Chemical Physics, Volume 154: Quantum Information and Computation for Chemistry, First Edition. Edited by Sabre Kais.

I. INTRODUCTION

The development and use of quantum computers for chemical applications has the potential for revolutionary impact on the way computing is done in the future [1–7]. Major challenge opportunities are abundant (see next fifteen chapters). One key example is developing and implementing quantum algorithms for solving chemical problems thought to be intractable for classical computers. Other challenges include the role of quantum entanglement, coherence, and superposition in photosynthesis and complex chemical reactions. Theoretical chemists have encountered and analyzed these quantum effects from the view of physical chemistry for decades. Therefore, combining results and insights from the quantum information community with those of the chemical physics community might lead to a fresh understanding of important chemical processes. In particular, we will discuss the role of entanglement in photosynthesis, in dissociation of molecules, and in the mechanism with which birds determine magnetic north. This chapter is intended to survey some of the most important recent results in quantum computation and quantum information, with potential applications in quantum chemistry. To start with, we give a comprehensive overview of the basics of quantum computing (the gate model), followed by introducing quantum simulation, where the phase estimation algorithm (PEA) plays a key role. Then we demonstrate how PEA combined with Hamiltonian simulation and multiplicative inversion can enable us to solve some types of linear systems of equations described by $A\vec{x} = \vec{b}$. Then our subject turns from gate model quantum computing (GMQC) to adiabatic quantum computing (AQC) and topological quantum computing, which have gained increasing attention in the recent years due to their rapid progress in both theoretical and experimental areas. Finally, applications of the concepts of quantum information theory are usually related to the powerful and counter intuitive quantum mechanical effects of superposition, interference, and entanglement.

Throughout history, man has learned to build tools to aid computation. From abacuses to digital microprocessors, these tools epitomize the fact that laws of physics support computation. Therefore, a natural question arises: "Which physical laws can we use for computation?" For a long period of time, questions such as this were not considered relevant because computation devices were built exclusively based on classical physics. It was not until the 1970s and 1980s when Feynmann [8], Deutsch [9], Benioff [10], and Bennett [11] proposed the idea of using quantum mechanics to perform calculation that the possibility of building a quantum computing device started to gain some attention.

What they conjectured then is what we call today a quantum computer. A quantum computer is a device that takes direct advantage of quantum mechanical phenomena such as superposition and entanglement to perform calculations [12]. Because they compute in ways that classical computers cannot, for certain problems quantum algorithms provide exponential speedups over their classical

counterparts. As an example, in solving problems related to factoring large numbers [13] and simulation of quantum systems [14–28], quantum algorithms are able to find the answer exponentially faster than classical algorithms. Recently, it has also been proposed that a quantum computer can be useful for solving linear systems of equations with exponential speedup over the best-known classical algorithms [29]. In the problem of factoring large numbers, the quantum exponential speedup is rooted in the fact that a quantum computer can perform discrete Fourier transform exponentially faster than classical computers [12]. Hence, any algorithm that involves Fourier transform as a subroutine can potentially be sped up exponentially on a quantum computer. For example, efficient quantum algorithms for performing discrete sine and cosine transforms using quantum Fourier transform have been proposed [30]. To illustrate the tremendous power of the exponential speedup with concrete numbers, consider the following example: the problem of factoring a 60-digit number takes a classical computer 3×10^{11} years (about 20 times the age of universe) to solve, while a quantum computer can be expected to factor a 60-digit number within 10^{-8} seconds. The same order of speedup applies for problems of quantum simulation.

In chemistry, the entire field has been striving to solve a number of "Holy Grail" problems since their birth. For example, manipulating matter on the atomic and molecular scale, economic solar splitting of water, the chemistry of consciousness, and catalysis on demand are all such problems. However, beneath all these problems is one common problem, which can be dubbed as the "Mother of All Holy Grails: exact solution of the Schrödinger equation. Paul Dirac pointed out that with the Schrödinger equation, "the underlying physical laws necessary for the mathematical theory of a large part of physics and the whole of chemistry are thus completely known and the difficulty is only that the exact application of these laws leads to equations much too complicated to be soluble" [31]. The problem of solving the Schrödinger equation is fundamentally hard [32,33] because as the number of particles in the system increases, the dimension of the corresponding Hilbert space increases exponentially, which entails exponential amount of computational resource.

Faced with the fundamental difficulty of solving the Schrödinger equations exactly, modern quantum chemistry is largely an endeavor aimed at finding approximate methods. *Ab initio* methods [34] (Hartree–Fock, Moller–Plesset, coupled cluster, Green's function, configuration interaction, etc.), semi-empirical methods (extended Huckel, CNDO, INDO, AM1, PM3, etc.), density functional methods [35] (LDA, GGA, hybrid models, etc.), density matrix methods [36], algebraic methods [37] (Lie groups, Lie algebras, etc.), quantum Monte Carlo methods [38] (variational, diffusion, Green's function forms, etc.), and dimensional scaling methods [39] are all products of such effort over the past decades. However, all the methods devised so far have to face the challenge of unreachable computational requirements as they are extended to higher accuracy to larger systems. For

example, in the case of full CI calculation, for N orbitals and m electrons there are $C_N^m \approx \frac{N^m}{m!}$ ways to allocate electrons among orbitals. Doing full configuration interaction (FCI) calculations for methanol (CH_3OH) using 6-31G (18 electrons and 50 basis functions) requires about 10^{17} configurations. This task is impossible on any current computer. One of the largest FCI calculations reported so far has about 10^9 configurations (1.3 billion configurations for Cr_2 molecules [40]).

However, due to exponential speedup promised by quantum computers, such simulation can be accomplished within only polynomial amount of time, which is reasonable for most applications. As we will show later, using the phase estimation algorithm, one is able to calculate eigenvalues of a given Hamiltonian H in time that is polynomial in $O(\log N)$, where N is the size of the Hamiltonian. So in this sense, quantum computation and quantum information will have enormous impact on quantum chemistry by enabling quantum chemists and physicists to solve problems beyond the processing power of classical computers.

The importance of developing quantum computers derives not only from the discipline of quantum physics and chemistry alone, but also from a wider context of computer science and the semiconductor electronics industry. Since 1946, the processing power of microprocessors has doubled every year simply due to the miniaturization of basic electronic components on a chip. The number of transistors on a single integrated circuit chip doubled every 18 months, which is a fact known as Moore's law. This exponential growth in the processing power of classical computers has spurred revolutions in every area of science and engineering. However, the trend cannot last forever. In fact, it is projected that by the year 2020 the size of a transistor would be on the order of a single atom. At that scale, classical laws of physics no longer hold and the behavior of the circuit components obeys laws of quantum mechanics, which implies that a new paradigm is needed to exploit the effects of quantum mechanics to perform computation, or in a more general sense, information processing tasks. Hence, the mission of quantum computing is to study how information can be processed with quantum mechanical devices as well as what kinds of tasks beyond the capabilities of classical computers can be performed efficiently on these devices.

Accompanying the tremendous promises of quantum computers are the experimental difficulties of realizing one that truly meets its above-mentioned theoretical potential. Despite the ongoing debate on whether building a useful quantum computer is possible, no fundamental physical principles are found to prevent a quantum computer from being built. Engineering issues, however, remain. The improvement and realization of quantum computers are largely interdisciplinary efforts. The disciplines that contribute to quantum computing, or more generally quantum information processing, include quantum physics, mathematics, computer science, solid-state device physics, mesoscopic physics, quantum devices, device technology, quantum optics, optical communication, and nuclear magnetic resonance (NMR), to name just a few.

A. Qubits and Gates

In general, we can think of information as something that can be encoded in the state of a physical system. If the physical system obeys classical laws of physics, such as a classical computer, the information stored there is of "classical" nature. To quantify information, the concept of *bit* has been introduced and defined as the basic unit of information. A *bit* of information stored in a classical computer is a value 0 or 1 kept in a certain location of the memory unit. The computer is able to measure the bit and retrieve the information without changing the state of the bit. If the bit is at the same state every time it is measured, it will yield the same results. A bit can also be copied and one can prepare another bit with the same state. A string of bits represents one single number.

All these properties of bits seem trivial but in the realm of quantum information processing, this is no longer true (Table I). The basic unit of quantum information is a *qubit*. Physically, a qubit can be represented by the state of a two-level quantum system of various forms, be it an ion with two accessible energy levels or a photon with two states of polarization. Despite the diverse physical forms that a qubit can take, for the most part the concept of "qubit" is treated as an abstract mathematical object. This abstraction gives us the freedom to construct a general theory of quantum computation and quantum information that does not depend on a specific system for its realization [12].

Unlike classical bits, a qubit can be not only in state $|0\rangle$ or $|1\rangle$, but also a superposition of both: $\alpha|0\rangle + \beta|1\rangle$. If a qubit is in a state of quantum superposition, a measurement will collapse the state to either one of its component states $|0\rangle$ or $|1\rangle$, which is a widely observed phenomenon in quantum physics. Suppose we repetitively do the following: prepare a qubit in the same state $\alpha|0\rangle + \beta|1\rangle$ and then measure it with respect to the basis state $\{|0\rangle, |1\rangle\}$. The measurement outcomes would most probably be different—we will get $|0\rangle$ in some measurements and $|1\rangle$ in the others—even the state of the qubit that is measured is identical each time. Furthermore, unlike classical bits that can be copied, a qubit cannot be copied due to the *no-cloning* theorem, which derives from a qubit's quantum mechanical nature

TABLE I
Comparison Between Classical Bits and Qubits

Classical Bit	Qubit
State 0 or 1	$|0\rangle$, $|1\rangle$, or superposition
Measurement does not change the state of the bit	Measurement changes the system
Deterministic result	Obtain different results with the same system
Can make a copy of bit (eavesdrop)	Cannot clone the qubit (security)
One number for a string bit	Store several numbers simultaneously due to superposition

(see Ref. [12], p. 24 for details). Such no-cloning property of a qubit has been used for constructing security communication devices, because a qubit of information is impossible to eavesdrop. In terms of information storage, since a qubit or an array of qubits could be in states of quantum superposition such as $\alpha_{00}|00\rangle + \alpha_{01}|01\rangle + \alpha_{10}|10\rangle + \alpha_{11}|11\rangle$, a string of qubits is able to store several numbers $\alpha_{00}, \alpha_{01}, \ldots$ simultaneously, while a classical string of bits can only represent a single number. In this sense, n qubits encode not n bits of classical information, but 2^n numbers. In spite of the fact that none of the 2^n numbers are efficiently accessible because a measurement will destroy the state of superposition, this exponentially large information processing space combined with the peculiar mathematical structure of quantum mechanics still implies the formidable potential in the performance of some of computational tasks exponentially faster than classical computers.

Now that we have introduced the basic processing units of quantum computers—the qubits, the next question is: How do we make them compute? From quantum mechanics we learned that the evolution of any quantum system must be *unitary*. That is, suppose a quantum computation starts with an initial state $|\Psi_{\text{initial}}\rangle$, then the final state of the computation $|\Psi_{\text{final}}\rangle$ must be the result of a unitary transformation U, which gives $|\Psi_{\text{final}}\rangle = U|\Psi_{\text{initial}}\rangle$. In classical computing, the basic components of a circuit that transforms a string $\{0, 1\}^n$ to another string $\{0, 1\}^m$ are called *gates*. Analogously, in quantum computing, a unitary transformation U that transforms a system from $|\Psi_{\text{initial}}\rangle$ to $|\Psi_{\text{final}}\rangle$ can also be decomposed into sequential applications of basic unitary operations called *quantum gates* (Table II). Experimentally, the implementation of a quantum gate largely depends on the device and technique used for representing a qubit. For example, if a qubit is physically represented by the state of a trapped ion, then the quantum gate is executed by an incident laser pulse that perturbs the trapped atom(s) and alters its state; if the qubit states are encoded in the polarization states of photons, then a quantum gate consists of optical components that interact with photons and alter their polarization states as they travel through the components.

If we use vectors to describe the state of a qubit, that is, using $|0\rangle$ to represent $(1, 0)^{\mathrm{T}}$ and $|1\rangle$ to represent $(0, 1)^{\mathrm{T}}$, a single-qubit quantum gate can be represented

TABLE II
Comparison Between Classical and Quantum Gates

Classical Logic Gates	Quantum Gates
Each gate corresponds to a mapping $\{0, 1\}^m \to \{0, 1\}^n$	Each quantum gate corresponds to a transformation $\|\Psi\rangle \to \|\Psi'\rangle$ or a rotation on the surface of Bloch sphere ([12], p. 15)
Nonunitary	Unitary
Irreversible	Reversible

using a 2×2 matrix. For example, a quantum NOT gate can be represented by the Pauli X matrix

$$U_{\text{NOT}} = X = \begin{pmatrix} 0 & 1 \\ 1 & 0 \end{pmatrix} \tag{1}$$

To see how this works, note that $X|0\rangle = |1\rangle$ and $X|1\rangle = |0\rangle$. Therefore, the sheer effect of applying X to a qubit is to flip its state from $|0\rangle$ to $|1\rangle$. This is just one example of single-qubit gates. Other commonly used gates include the Hadamard gate H, Z rotation gate, phase gate S, and $\frac{\pi}{8}$ gate T:

$$H = \frac{1}{\sqrt{2}} \begin{pmatrix} 1 & 1 \\ 1 & -1 \end{pmatrix}, \quad S = \begin{pmatrix} 1 & 0 \\ 0 & i \end{pmatrix}, \quad T = \begin{pmatrix} 1 & 0 \\ 0 & e^{i\pi/4} \end{pmatrix} \tag{2}$$

If a quantum gate involves two qubits, then it is represented by a 4×4 matrix. The state of a two-qubit system is generally in form of $\alpha_{00}|00\rangle + \alpha_{01}|01\rangle + \alpha_{10}|10\rangle + \alpha_{11}|11\rangle$, which can be written as a vector $(\alpha_{00}, \alpha_{01}, \alpha_{10}, \alpha_{11})^{\text{T}}$. In matrix form, the CNOT gate is defined as

$$U_{\text{CNOT}} = \begin{pmatrix} 1 & 0 & 0 & 0 \\ 0 & 1 & 0 & 0 \\ 0 & 0 & 0 & 1 \\ 0 & 0 & 1 & 0 \end{pmatrix} \tag{3}$$

It is easy to verify that applying CNOT gate to a state $|\Psi_0\rangle = \alpha_{00}|00\rangle + \alpha_{01}|01\rangle + \alpha_{10}|10\rangle + \alpha_{11}|11\rangle$ results in a state

$$U_{\text{CNOT}}|\Psi_0\rangle = \alpha_{00}|00\rangle + \alpha_{01}|01\rangle + \alpha_{10}|11\rangle + \alpha_{11}|10\rangle \tag{4}$$

Hence, the effect of a CNOT gate is equivalent to a conditional X gate: If the first qubit is in $|0\rangle$, then the second qubit remains intact; on the other hand, if the first qubit is in $|1\rangle$, then the second qubit is flipped. Generally, the first qubit is called the *control* and the second is the *target*.

In classical computing, an arbitrary mapping $\{0, 1\}^n \to \{0, 1\}^m$ can be executed by a sequence of basic gates such as AND, OR, NOT, and so on. Similarly in quantum computing, an arbitrary unitary transformation U can also be decomposed as a product of basic quantum gates. A complete set of such basic quantum gates is a *universal gate set*. For example, Hadamard, phase, CNOT, and $\pi/8$ gates form a universal gate set ([12], p. 194).

Now that we have introduced the concepts of qubits and quantum gates and compared them with their classical counterpart, we can see that they are the very building blocks of a quantum computer. However, it turns out that having qubits and executable universal gates is not enough for building a truly useful quantum

computer that delivers its theoretical promises. So what does it really take to build such a quantum computer? A formal answer to this question is the following seven criteria proposed by DiVincenzo [41]:

- A scalable physical system with well-characterized qubits.
- The ability to initialize the state of the qubits to a simple fiducial state.
- Long (relative) decoherence times, much longer than the gate operation time.
- A universal set of quantum gates.
- A qubit-specific measurement capability.
- The ability to inter convert stationary and flying qubits.
- The ability to faithfully transmit flying qubits between specified locations.

For a detailed review of state-of-the-art experimental implementation based on the preceding criteria, refer to Ref. [42]. The take-home message is that it is clear that we can gain some advantage by storing, transmitting, and processing information encoded in systems that exhibit unique quantum properties, and a number of physical systems are currently being developed for quantum computation. However, it remains unclear which technology, if any, will ultimately prove successful in building a scalable quantum computer.

B. Circuits and Algorithms

Just as in classical computing, logic gates are cascaded to form a circuit. A *quantum circuit* is a sequence of quantum gates. When an algorithm needs to be implemented with a quantum computer, it must first be translated to a quantum circuit in order to be executed on the quantum hardware (qubits). Figure 1 is an example of a quantum circuit. Each horizontal line represents a qubit and every box on the line is a quantum gate applied on that qubit. If the box is connected with a vertical line that joins it to the line(s) with solid circles, then the box is a controlled gate operation and the qubit(s) that it is joined to are the control qubit(s). Just like a CNOT gate, only when the control qubit (s) is (are all) in $|1\rangle$ state will the controlled operation be applied onto the target qubit.

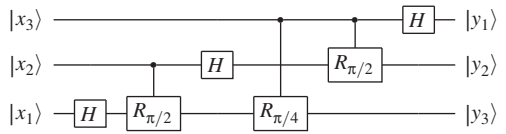

Figure 1. Quantum circuit for quantum Fourier transform on the quantum state $|x_1, x_2, x_3\rangle$. Starting from the left, the first gate is a Hadamard gate H that acts on the qubit in the state $|x_1\rangle$, and the second gate is a $|x_2\rangle$-controlled phase rotation $R_\theta(a|0\rangle + b|1\rangle) \rightarrow (a|0\rangle + be^{i\theta}|1\rangle)$ on qubit $|x_1\rangle$, where $\theta = \pi/2$. The rest of the circuit can be interpreted in the same fashion.

C. Teleportation

Quantum teleportation exploits some of the most basic and unique features of quantum mechanics, which is quantum entanglement, essentially implies an intriguing property that two quantum correlated systems cannot be considered independent even if they are far apart. The dream of teleportation is to be able to travel by simply reappearing at some distant location. Teleportation of a quantum state encompasses the complete transfer of information from one particle to another. The complete specification of a quantum state of a system generally requires an infinite amount of information, even for simple two-level systems (qubits). Moreover, the principles of quantum mechanics dictate that any measurement on a system immediately alters its state, while yielding at most one bit of information. The transfer of a state from one system to another (by performing measurements on the first and operations on the second) might therefore appear impossible. However, it was shown that the property of entanglement in quantum mechanics, in combination with classical communication, can be used to teleport quantum states. Although teleportation of large objects still remains a fantasy, quantum teleportation has become a laboratory reality for photons, electrons, and atoms [43–52].

More precisely, quantum teleportation is a quantum protocol by which the information on a qubit A is transmitted exactly (in principle) to another qubit B. This protocol requires a conventional communication channel capable of transmitting two classical bits, and an entangled pair (B, C) of qubits, with C at the location of origin with A and B at the destination. The protocol has three steps: measure A and C jointly to yield two classical bits; transmit the two bits to the other end of the channel; and use the two bits to select one of the four ways of recovering B [53,54].

Efficient long-distance quantum teleportation is crucial for quantum communication and quantum networking schemes. Ursin and coworkers [55] have performed a high-fidelity teleportation of photons over a distance of 600 m across the River Danube in Vienna, with the optimal efficiency that can be achieved using linear optics. Another exciting experiment in quantum communication has also been done with one photon that is measured locally at the Canary Island of La Palma, whereas the other is sent over an optical free-space link to Tenerife, where the Optical Ground Station of the European Space Agency acts as the receiver [55,56]. This exceeds previous free-space experiments by more than an order of magnitude in distance, and is an essential step toward future satellite-based quantum communication.

Recently, we have proposed a scheme for implementing quantum teleportation in a three-electron systems [52]. For more electrons, using Hubbard Hamiltonian, in the limit of the Coulomb repulsion parameter for electrons on the same site $U \to +\infty$, there is no double occupation in the magnetic field; the system is reduced to the Heisenberg model. The neighboring spins will favor the anti parallel

configuration for the ground state. If the spin at one end is flipped, then the spins on the whole chain will be flipped accordingly due to the spin–spin correlation. Such that the spins at the two ends of the chain are entangled, a spin entanglement can be used for quantum teleportation, and the information can be transferred through the chain. This might be an exciting new direction for teleportation in molecular chains [57].

II. QUANTUM SIMULATION

A. Introduction

As already mentioned, simulating quantum systems by exact solution of the Schrödinger equation is a fundamentally hard task that the quantum chemistry community has been trying to tackle for decades with only approximate approaches. The key challenges of quantum simulation include the following (see next five chapters) [28]:

1. Isolate qubits in physical systems. For example, in a photonic quantum computer simulating a hydrogen molecule, the logical states $|0\rangle$ and $|1\rangle$ correspond to horizontal $|H\rangle$ and vertical $|V\rangle$ polarization states [58].
2. Represent the Hamiltonian H. This is to write H as a sum of Hermitian operators, each to be converted into unitary gates under the exponential map.
3. Prepare the states $|\psi\rangle$. By direct mapping, each qubit represents the fermionic occupation state of a particular orbital. Fock space of the system is mapped onto the Hilbert space of qubits.
4. Extract the energy E.
5. Read out the qubit states.

A technique to accomplish challenge 2 in a robust fashion is presented in Section II.B.2. Challenge 4 is accomplished using the phase estimation quantum algorithm (see details in Section II.B). Here, we can mention some examples of algorithms and their corresponding quantum circuits that have been implemented experimentally: (a) the IBM experiment, which factors the number 15 with nuclear magnetic resonance (NMR) (for details see Ref. [59]); (b) using quantum computers for quantum chemistry [58].

B. Phase Estimation Algorithm

The phase estimation algorithm (PEA) takes advantage of quantum Fourier transform ([12], see chapter by Gaitan and Nori) to estimate the phase φ in the eigenvalue $e^{2\pi i\varphi}$ of a unitary transformation U. For a detailed description of the algorithm, refer to Ref. [60]. The function that the algorithm serves can be summarized as the

following: Let $|u\rangle$ be an eigenstate of the operator U with eigenvalue $e^{2\pi i\varphi}$. The algorithm starts with a two-register system (a *register* is simply a group of qubits) in the state $|0\rangle^{\otimes t}|u\rangle$. Suppose the transformation U^{2^k} can be efficiently performed for integer k, then this algorithm can efficiently obtain the state $|\tilde{\varphi}\rangle|u\rangle$, where $|\tilde{\varphi}\rangle$ accurately approximates φ to $t - \lceil \log(2 + \frac{1}{2\epsilon}) \rceil$ bits with probability of at least $1 - \epsilon$.

1. General Formulation

The generic quantum circuit for implementing PEA is shown in Fig. 2. Section 5.2 of Ref. [12] presents a detailed account of how the circuit functions mathematically to yield the state $|\tilde{\varphi}\rangle$, which encodes the phase φ. Here we focus on its capability of finding the eigenvalues of a Hermitian matrix, which is of great importance in quantum chemistry where one often would like to find the energy spectrum of a Hamiltonian.

Suppose we let $U = e^{iAt_0/2^t}$ for some Hermitian matrix A, then $e^{iAt_0}|u_j\rangle = e^{i\lambda_j t}|u_j\rangle$, where λ_j and $|u_j\rangle$ are the j-th eigenvalue and eigenvector of matrix A. Furthermore, we replace the initial state $|u\rangle$ of register b (Fig. 2) with an arbitrary vector $|b\rangle$ that has a decomposition in the basis of the eigenvectors of A: $|b\rangle = \sum_j^n \beta_j |u_j\rangle$. Then the major steps of the algorithm can be summarized as the following.

1. Transform the t-qubit register C (Fig. 2) from $|0\rangle^{\otimes t}$ to $\frac{1}{\sqrt{2^t}} \sum_{\tau=0}^{2^t-1} |\tau\rangle$ state by applying Hadamard transform on each qubit in register C.
2. Apply the U^{2^k} gates to the register b, where each U^{2^k} gate is controlled by the $(k-1)$th qubit of the register C from bottom. This series of controlled operations transforms the state of the two-register system from $\frac{1}{\sqrt{2^t}} \sum_{\tau=0}^{2^t-1} |\tau\rangle \otimes |b\rangle$ to $\frac{1}{\sqrt{2^t}} \sum_{\tau=0}^{2^t-1} |\tau\rangle \sum_{j=1}^{n} e^{i\lambda_j \tau t/2^t} \beta_j |u_j\rangle$.
3. Apply inverse Fourier transform $\mathrm{FT}^\dagger$ to the register C. Because every basis state $|\tau\rangle$ will be transformed to $\frac{1}{\sqrt{2^t}} \sum_{k=0}^{2^t-1} e^{-2\pi i \tau k/2^t} |k\rangle$ by $\mathrm{FT}^\dagger$, the final

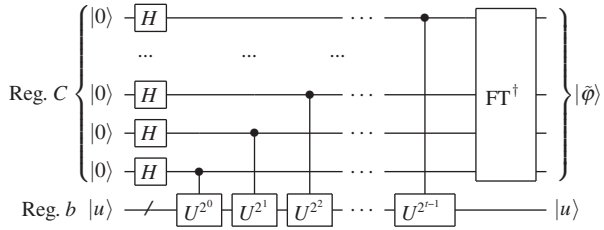

Figure 2. Schematic of the quantum circuit for phase estimation. The quantum wire with a "/" symbol represents a register of qubits as a whole. $\mathrm{FT}^\dagger$ represents inverse Fourier transform, whose circuit is fairly standard ([12], see chapter by Gaitan and Nori).

state of the PEA is proportional to $\sum_{k=0}^{2^t-1}\sum_{j=1}^{n} e^{i(\lambda_j t_0 - 2\pi k)\tau/2^t}\beta_j|k\rangle|u_j\rangle$. Due to a well-known property of the exponential sum, in which sums of the form $\sum_{k=0}^{N-1}\exp(2\pi ik\frac{r}{N})$ vanish unless $r = 0 \bmod N$, the values of k are concentrated on those whose value is equal or close to $\frac{t_0}{2\pi}\lambda_j$. If we let $t_0 = 2\pi$, the final state of system is $\sum_j \beta_j|\tilde{\lambda}_j\rangle|u_j\rangle$ up to a normalization constant.

In particular, if we prepare the initial state of register b to be one of matrix A's eigenvector $|u_i\rangle$, according to the procedure listed above, the final state of the system will become $|\tilde{\lambda}_i\rangle|u_i\rangle$ up to a constant. Hence, for any $|u_i\rangle$ that we can prepare, we can find the eigenvalue λ_j of A corresponding to $|u_i\rangle$ using a quantum computer. Most importantly, it has been shown that [17] quantum computers are able to solve the eigenvalue problem significantly more efficiently than classical computers.

2. *Implementation of Unitary Transformation U*

Phase estimation algorithm is often referred to as a *black box* algorithm because it assumes that the unitary transformation U and its arbitrary powers can be implemented with basic quantum gates. However, in many cases U has a structure that renders finding the exact decomposition $U = U_1U_2...U_m$ either impossible or very difficult. Therefore, we need a robust method for finding approximate circuit decompositions of unitary operators U with minimum cost and minimum fidelity error.

Inspired by the optimization nature of the circuit decomposition problem, Daskin and Kais [61,62] have developed an algorithm based on group leader optimization technique for finding a circuit decomposition $U = U_1U_2...U_m$ with minimum gate cost and fidelity error for a particular U. Hence, there are two factors that need to be optimized within the optimization: the error and the cost of the circuit. The costs of a one-qubit gate and a control gate (two-qubit gate) are defined as 1 and 2, respectively. Based on these two definitions, the costs of other quantum gates can be deduced. In general, the minimization of the error to an acceptable level is more important than the cost in order to get more reliable results in the optimization process. The circuit decompositions for $U = e^{iAt}$ presented in Fig. 3b for the particular instance of A in Eq. (6) are found by the algorithm such that the error $||U' - U||$ and the cost of U' are both minimized.

3. *Group Leaders Optimization Algorithm*

The group leaders optimization algorithm (GLOA) described in more detail in Refs [61,62] is a simple and effective global optimization algorithm that models the influence of leaders in social groups as an optimization tool. The algorithm starts with dividing the randomly generated solution population into several disjunct groups and assigning for each group a leader (the best candidate solution inside

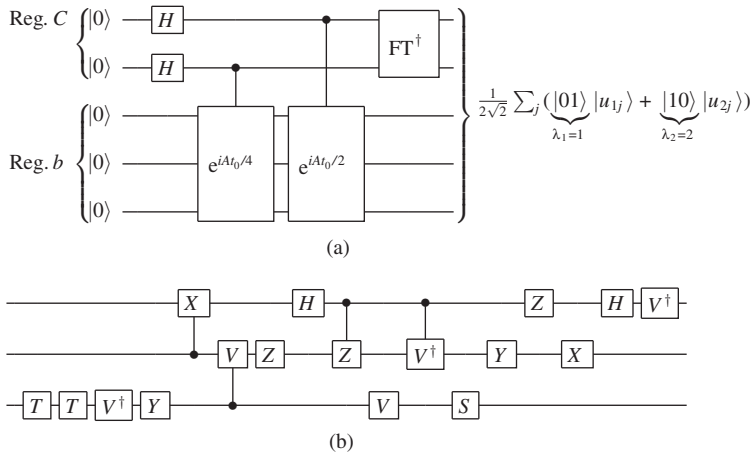

Figure 3. Quantum circuit for estimating the eigenvalues of A, which is the 8×8 matrix shown in Eq. (6). (**a**) The overall circuit implementing the phase estimation algorithm. (**b**) Decomposition of the gate $e^{iA\frac{t_0}{4}}$ in terms of basic gates.

the group). The algorithm basically is built on two parts: mutation and parameter transfer. In the mutation part, a candidate solution (a group member that is not leader) is mutated by using some part of its group leader, some random part, and some part of this member itself. This mutation is formulated as

$$\begin{aligned} \text{new member} &= r_1 \text{ part of the member} \\ &\cup\ r_2 \text{ part of its leader} \\ &\cup\ r_3 \text{ part of random} \end{aligned} \tag{5}$$

where r_1, r_2, and r_3 determine the rates of the member, the group leader, and the newly created random solution into the newly formed member, and they sum to 1. The values of these rates are assigned as $r_1 = 0.8$ and $r_2 = r_3 = 0.1$. The mutation for the values of the all angles in a numerical string is done according to the arithmetic expression: $\text{angle}_{\text{new}} = r_1 \times \text{angle}_{\text{old}} + r_2 \times \text{angle}_{\text{leader}} + r_3 \times \text{angle}_{\text{random}}$, where $\text{angle}_{\text{old}}$, the current value of an angle, is mutated: $\text{angle}_{\text{new}}$, the new value of the angle, is formed by combining a random value and the corresponding leader of the group of the angle and the current value of the angle with the coefficients r_1, r_2, and r_3. The mutation for the rest of the elements in the string means the replacement of its elements by the corresponding elements of the leader and a newly generated random string with the rates r_2 and r_3. In the second part of the algorithm, these disjoint groups communicate with each other by transferring some parts of their members. This step is called parameter transfer. In

this process, some random part of a member is replaced with the equivalent part of a random member from a different group. The amount of this communication process is limited with some parameter that is set to $\frac{4\times \max_{\text{gates}}}{2} - 1$, where the numerator is the number of variables forming a numeric string in the optimization. During the optimization, the replacement criterion between a newly formed member is and an existing member is defined as follows: If a new member formed by a mutation or a parameter transfer operation gives less error-prone solution to the problem than the corresponding member, or they have the same error values but the cost of the new member is less than this member, then the new member takes the former one's place as a candidate solution; otherwise, the newly formed member is disregarded.

4. Numerical Example

In order to demonstrate how PEA finds the eigenvalues of a Hermitian matrix, here we present a numerical example. We choose A as a Hermitian matrix with the degenerate eigenvalues $\lambda_i = 1, 2$ and corresponding eigenvectors $|u_{11}\rangle = |++\rangle, |u_{12}\rangle = |+-\rangle, |u_{13}\rangle = |-+\rangle, |u_{14}\rangle = |--\rangle, |u_{21}\rangle = |+-\rangle, |u_{22}\rangle = |--\rangle, |u_{23}\rangle = |-+\rangle, |u_{24}\rangle = |++\rangle$:

$$A = \begin{pmatrix} 1.5 & -0.25 & -0.25 & 0 & -0.25 & 0 & 0 & 0.25 \\ -0.25 & 1.5 & 0 & -0.25 & 0 & -0.25 & 0.25 & 0 \\ -0.25 & 0 & 1.5 & -0.25 & 0 & 0.25 & -0.25 & 0 \\ 0 & -0.25 & -0.25 & 1.5 & 0.25 & 0 & 0 & -0.25 \\ -0.25 & 0 & 0 & 0.25 & 1.5 & -0.25 & -0.25 & 0 \\ 0 & -0.25 & 0.25 & 0 & -0.25 & 1.5 & 0 & -0.25 \\ 0 & 0.25 & -0.25 & 0 & -0.25 & 0 & 1.5 & -0.25 \\ 0.25 & 0 & 0 & -0.25 & 0 & -0.25 & -0.25 & 1.5 \end{pmatrix} \tag{6}$$

Here $|+\rangle = \frac{1}{\sqrt{2}}(|0\rangle + |1\rangle)$ and $|-\rangle = \frac{1}{\sqrt{2}}(|0\rangle - |1\rangle)$ represent the Hadamard states. Furthermore, we let $\vec{b} = (1, 0, 0, 0, 0, 0, 0, 0)^{\mathrm{T}}$. Therefore, $|b\rangle = |000\rangle = \sum_j \beta_j |u_j\rangle$ and each $\beta_j = \frac{1}{2\sqrt{2}}$. Figure 3 shows the circuit for solving the 8×8 linear system. The register C is first initialized with Walsh–Hadamard transformation and then used as the control register for Hamiltonian simulation e^{iAt_0} on the register B. The decomposition of the two-qubit Hamiltonian simulation operators in terms of basic quantum circuits is achieved using group leader optimization algorithm [61,62]. The final state of system is $\sum_j \beta_j |\lambda_j\rangle |u_j\rangle = \frac{1}{2\sqrt{2}} \sum_{i=1}^{4} (|01\rangle |u_{1i}\rangle + |10\rangle |u_{2i}\rangle)$, which encodes both eigenvalues 1 (as $|01\rangle$) and 2 (as $|10\rangle$) in register C (Fig. 3).

5. *Simulation of the Water Molecule*

Wang et al.'s algorithm [19] can be used to obtain the energy spectrum of molecular systems such as water molecule based on the multiconfigurational self-consistent field (MCSCF) wave function. By using a MCSCF wave function as the initial guess, the excited states are accessible. The geometry used in the calculation is near the equilibrium geometry (OH distance $R = 1.8435a_0$ and the angle HOH = 110.57°). With a complete active space type MCSCF method for the excited-state simulation, the CI space is composed of 18 CSFs, which requires the use of five qubits to represent the wave function. The unitary operator for this Hamiltonian can be formulated as

$$\hat{U}_{\mathrm{H_2O}} = \mathrm{e}^{i\tau(E_{\max}-\mathcal{H})t} \tag{7}$$

where τ is given as

$$\tau = \frac{2\pi}{E_{\max} - E_{\min}} \tag{8}$$

$E_{\max}$ and $E_{\min}$ are the expected maximum and minimum energies. The choice of $E_{\max}$ and $E_{\min}$ must cover all the eigenvalues of the Hamiltonian to obtain the correct results. After finding the phase ϕ_j from the phase estimation algorithm, the corresponding final energy E_j is found from the following expression:

$$E_j = E_{\max} - \frac{2\pi\phi_j}{\tau} \tag{9}$$

Because the eigenvalues of the Hamiltonian of the water molecule are between $-80 \pm \epsilon$ and $-84 \pm \epsilon$ ($\epsilon \leq 0.1$), taking $E_{\max} = 0$ and $E_{\min} = -200$ gives the following:

$$\hat{U} = \mathrm{e}^{\frac{-i2\pi H}{200}t} \tag{10}$$

Figure 4 shows the circuit diagram for this unitary operator generated by using the optimization algorithm and procedure as defined. The cost of the circuit is

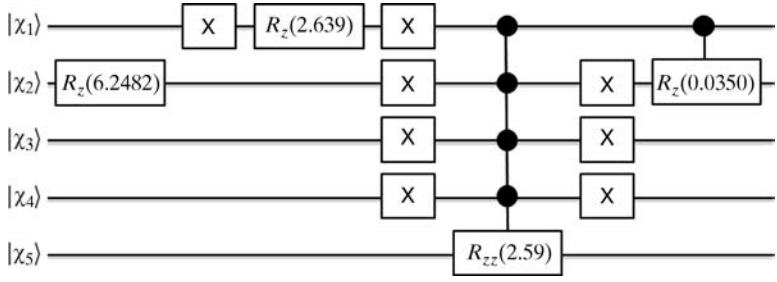

Figure 4. The circuit design for the unitary propagator of the water molecule.

TABLE III
Energy Eigenvalues of the Water Molecule

Phase	Found Energy	Exact Energy
0.4200	−84.0019	−84.0021
0.4200	−84.0019	−83.4492
0.4200	−84.0019	−83.0273
0.4200	−84.0019	−82.9374
0.4200	−84.0019	−82.7719
0.4200	−84.0019	−82.6496
0.4200	−84.0019	−82.5252
0.4200	−84.0019	−82.4467
0.4144	−82.8884	−82.3966
0.4144	−82.8884	−82.2957
0.4144	−82.8884	−82.0644
0.4144	−82.8884	−81.9872
0.4144	−82.8884	−81.8593
0.4144	−82.8884	−81.6527
0.4144	−82.8884	−81.4592
0.4144	−82.8884	−81.0119
0.4122	−82.4423	−80.9065
0.4122	−82.4423	−80.6703

44, which is found by summing up the cost of each gates in the circuit. Because we take $E_{\max}$ as zero, this deployment does not require any extra quantum gate for the implementation within the phase estimation algorithm. The simulation of this circuit within the iterative PEA results in the phase and energy eigenvalues given in Table III: The left two columns are, respectively, the computed phases and the corresponding energies, while the rightmost column of the matrix is the eigenvalues of the Hamiltonian of the water molecule (for each value of the phase, the PEA is run 20 times).

III. ALGORITHM FOR SOLVING LINEAR SYSTEMS $A\vec{x} = \vec{b}$

A. General Formulation

The algorithm solves a problem where we are given a Hermitian s-sparse $N \times N$ matrix A and a unit vector $\vec{b}$ (Fig. 5). Suppose we would like to find $\vec{x}$ such that $A\vec{x} = \vec{b}$. The algorithm can be summarized as the following major steps [29]:

1. Represent the vector $\vec{b}$ as a quantum state $|b\rangle = \sum_{i=1}^{N} b_i |i\rangle$ stored in a quantum register (termed *register b*). In a separate quantum register (termed *register C*) of t qubits, initialize the qubits by transforming the register to state $|\Psi\rangle^C$ from $|0\rangle$ up to error ϵ_Ψ.

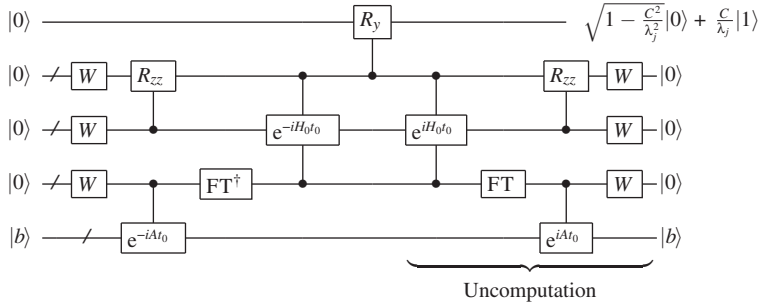

Figure 5. Generic quantum circuit for implementing the algorithm for solving linear systems of equations. The registers from the bottom of the circuit diagram upwards are, respectively, registers b, C, m, and l. The qubit on the top of the figure represents the ancilla bit.

2. Apply the conditional Hamiltonian evolution $\sum_{\tau=0}^{T-1} |\tau\rangle\langle\tau|^C \otimes e^{iA\tau t_0/T}$ up to error ϵ_H.
3. Apply quantum inverse Fourier transform to the register C. Denote the basis states after quantum Fourier transform as $|k\rangle$. At this stage in the superposition state of both registers, the amplitudes of the basis states are concentrated on k values that approximately satisfy $\lambda_k \approx \frac{2\pi k}{t_0}$, where λ_k is the kth eigenvalue of the matrix A.
4. Add an ancilla qubit and apply conditional rotation on it, controlled by the register C with $|k\rangle \approx |\lambda_k\rangle$. The rotation transforms the qubit to $\sqrt{1-\frac{C^2}{\lambda_j^2}}|0\rangle + \frac{C}{\lambda_j}|1\rangle$. This key step of the algorithm involves finding the reciprocal of the eigenvalue λ_j quantum mechanically, which is not a trivial task on its own. Now we assume that we have methods readily available to find the reciprocal of the eigenvalues of matrix A and store them in a quantum register.
5. Uncompute the register b and C by applying Fourier transform on register C followed by the complex conjugates of same conditional Hamiltonian evolution as in step 2 and Walsh–Hadamard transform as in the first step.
6. Measure the ancilla bit. If it returns 1, the register b of the system is in the state $\sum_{j=1}^{n} \beta_j {\lambda_j}^{-1} |u_j\rangle$ up to a normalization factor, which is equal to the solution $|x\rangle$ of the linear system $A\vec{x} = \vec{b}$. Here $|u_j\rangle$ represents the jth eigenvector of the matrix A and let $|b\rangle = \sum_{i=1}^{n} \beta_j |u_j\rangle$.

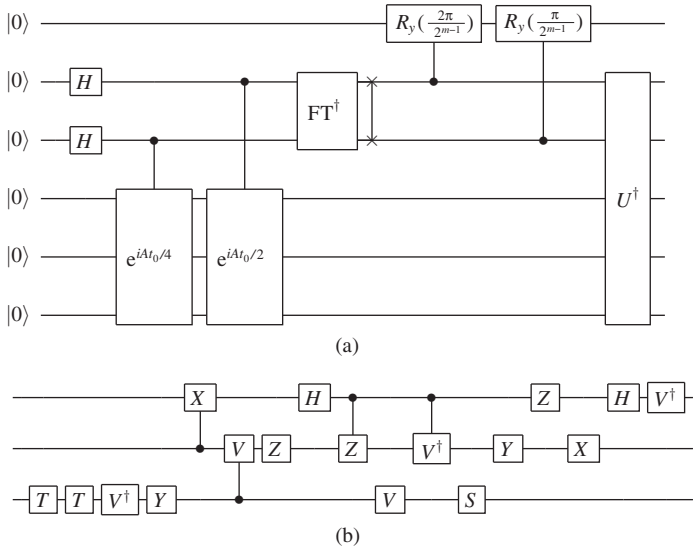

Figure 6. Quantum circuit for solving $A\vec{x} = \vec{b}$ with $A_{8\times 8}$ being the matrix shown in Eq. (6). (**a**) The overall circuit. From bottom up are the two qubits for $|b\rangle$, zeroth qubit in register C for encoding the eigenvalue, first qubit in register C for eigenvalue, and ancilla bit. $U^\dagger$ represents uncomputation. (**b**) Decomposition of the gate $e^{iA\frac{t_0}{4}}$ in terms of basic gates.

B. Numerical Example

For this example we choose A as the same Hermitian matrix as the one in Eq. (6). Furthermore, we let $\vec{b} = (1, 0, 0, 0, 0, 0, 0, 0)^{\mathrm{T}}$. Therefore, $|b\rangle = |000\rangle = \sum_j \beta_j |u_j\rangle$ and each $\beta_j = \frac{1}{2\sqrt{2}}$. To compute the reciprocals of the eigenvalues, a quantum *swap* gate is used (Fig. 6) to exchange the values of the zeroth and first qubit. By exchanging the values of the qubits, one inverts an eigenvalue of A, say 1 (encoded with $|01\rangle$), to $|10\rangle$, which represents 2 in binary form. In the same way, the eigenvalue 2 ($|10\rangle$) can be inverted to 1 $|01\rangle$.

Figure 6 shows the circuit for solving the 8×8 linear system. The register C is first initialized with Walsh–Hadamard transformation and then used as the control register for Hamiltonian simulation e^{iAt_0} on the register B. The decomposition of the two-qubit Hamiltonian simulation operators in terms of basic quantum circuits is achieved using group leader optimization algorithm [61,62].

The final state of system, conditioned on obtaining $|1\rangle$ in the ancilla bit, is $\frac{1}{2\sqrt{10}}(6|000\rangle + |001\rangle + |010\rangle + |100\rangle - |111\rangle)$, which is proportional to the exact solution of the system $\vec{x} = (0.75, 0.125, 0.125, 0, 0.125, 0, 0, -0.125)^{\mathrm{T}}$.

IV. ADIABATIC QUANTUM COMPUTING

The model of adiabatic quantum computation (AQC) was initially suggested by Farhi, Goldstone, Gutman, and Sisper [63] for solving some classical optimization problems. Several years after the proposition of AQC, Aharonov, Dam, Kempe, Landau, Lloyd, and Regev [64] assessed its computational power and established that the model of AQC is polynomially equivalent to the standard gate model quantum computation. Nevertheless, this model provides a completely different way of constructing quantum algorithms and reasoning about them. Therefore, it is seen as a promising approach for the discovery of substantially new quantum algorithms.

Prior to the work by Aharonov et al. [64], it had been known that AQC can be simulated by GMQC [65,66]. The equivalence between AQC and GMQC is then proven by showing that standard quantum computation can be efficiently simulated by adiabatic computation using 3-local Hamiltonians [64]. While the construction of three-particle Hamiltonians is sufficient for substantiating the theoretical results, it is technologically difficult to realize. Hence, significant efforts have been devoted to simplifying the universal form of Hamiltonian to render it feasible for physical implementation [64,67–70].

From the experimental perspective, current progress [71,72] in devices based on superconducting flux qubits has demonstrated the capability to implement Hamiltonian of the form $\Sigma_i h_i \sigma_i^z + \Sigma_i \Delta_i \sigma_i^x + \Sigma_{i,j} J_{ij} \sigma_i^z \sigma_j^z$. However, this is not sufficient for constructing a universal adiabatic quantum computer [71]. It is shown [68] that this Hamiltonian can be rendered universal by simply adding a tunable 2-local transverse $\sigma^x\sigma^x$ coupling. Once tunable $\sigma^x\sigma^x$ is available, all the other 2-local interactions such as $\sigma^z\sigma^x$ and $\sigma^x\sigma^z$ can be reduced to sums of single σ^x, σ^z spins and $\sigma^x\sigma^x$, $\sigma^z\sigma^z$ couplings via a technique called *Hamiltonian gadgets*. In Section IV.3, we will present a more detailed review of this subject.

A. Hamiltonians of *n*-Particle Systems

In the standard GMQC, the state of n qubits evolves in discrete time steps by unitary operations. Physically, however, the evolution is continuous and is governed by the *Schrödinger equation*: $-i\frac{\mathrm{d}}{\mathrm{d}t}|\psi(t)\rangle = H(t)|\psi(t)\rangle$, where $|\psi(t)\rangle$ is the state of n qubits at time t and $H(t)$ is a Hermitian $2^n \times 2^n$ matrix called the *Hamiltonian* operating on the n-qubit system; it governs the dynamics of the system. The fact that it is Hermitian derives from the unitary property of the discrete time evolution of the quantum state from t_1 to a later time t_2. In some context, the eigenvalues of Hamiltonians are referred to as *energy levels*. The *ground-state energy* of a Hamiltonian is its lowest eigenvalue and the corresponding

eigenvector(s) are the *ground state(s)*. The *spectral gap* $\Delta(H)$ of a Hamiltonian H is defined as the difference between lowest eigenvalue of H and its second lowest eigenvalue.

We say that a Hamiltonian H is k-local if H can be written as $\sum_A H^A$ where A runs over all subsets of k particles. In other words, H^A is a tensor product of a Hamiltonian on A with identity on the particles outside A. Note that although a k-local Hamiltonian H operating on n qubits dwells in the Hilbert space of dimension 2^n, it can be described by $2^{2k}n^k = \text{poly}(n)$ numbers.

B. The Model of Adiabatic Computation

To perform useful computations, the model of AQC hinges on a well-known principle called adiabatic theorem [73,74]. Consider a system with a time-dependent Hamiltonian $H(s)$, where $s \in [0, 1]$ is the normalized time parameter. The system is initialized at $t = 0$ in the ground state of $H(0)$ (assuming that for any s the ground state of $H(s)$ is unique). Then we let the system evolve according to the Hamiltonian $H(t/T)$ from time $t = 0$ to T. We refer to such process as an *adiabatic evolution* according to H for time T. The adiabatic theorem ensures that for T sufficiently large, the final state of the system is very close to the ground state of $H(1)$. The minimum T required for this process is a function of the minimum spectral gap $\Delta(H(s))$, as is stated in the adiabatic theorem:

Theorem 1 (The Adiabatic Theorem [75]) *Let H_{init} and H_{final} be two Hamiltonians acting on a quantum system and consider the time-dependent Hamiltonian $H(s) := (1 - s)H_{\text{init}} + sH_{\text{final}}$. Assume that for all s, $H(s)$ has a unique ground state. Then for any fixed $\delta > 0$, if*

$$T \geq \Omega\left(\frac{||H_{\text{final}} - H_{\text{init}}||^{1+\delta}}{\epsilon^{\delta} \min_{s\in[0,1]}\{\Delta^{2+\delta}(H(s))\}}\right) \tag{11}$$

then the final state of an adiabatic evolution according to H for time T (with an approximate setting of global phase) is ϵ-close in l_2-norm to the ground state of H_{final}. The matrix norm is the spectral norm $||H|| := \max_w ||Hw||/||w||$.

Based on Eq. (11), a reasonable definition of the running time of the adiabatic algorithm is $T \cdot \max_s ||H(s)||$, because we must take into account the physical trade-off between time and energy [64]. (The solution to the Schrödinger equation remains the same if time is divided by some factor and at the same time the Hamiltonian is multiplied by the same factor.) Hence, in order to show that an adiabatic algorithm is efficient, it is enough to use Hamiltonian of at most poly(n) norm, and show that for all $s \in [0, 1]$ the spectral gap $\Delta(H(s))$ is at least inverse polynomial in n.

C. Hamiltonian Gadgets

A perturbation gadget or simply a gadget Hamiltonian refers to a Hamiltonian construction invented by Kempe, Kitaev, and Regev [67] first used to approximate the ground states of k-body Hamiltonians using the ground states of two-body Hamiltonians. Gadgets have been used and/or extended by several authors including Oliveira and Terhal [76–79]. Recent results have been reviewed in the article by Wolf [80]. Gadgets have a range of applications in quantum information theory, many-body physics, and are mathematically interesting to study in their own right. They have recently come to occupy a central role in the solution of several important and long-standing problems in quantum information theory. Kempe, Kitaev, and Regev [81] introduced these powerful tools to show that finding the ground state of a 2-local system (i.e., a system with at most two-body interactions) is in the same complexity class QMA as finding the ground-state energy of a system with k-local interactions. This was done by introducing a gadget that reduced 3-local to 2-local interactions. Oliveira and Terhal [76] exploited the use of gadgets to manipulate Hamiltonians acting on a 2D lattice. The work in [76,81] was instrumental in finding simple spin models with a QMA-complete ground-state energy problem [78]. Aside from complexity theory, Hamiltonian gadget constructions have important application in the area of adiabatic quantum computation [76,77,81]. The application of gadgets extends well beyond the scope mentioned here.

V. TOPOLOGICAL QUANTUM COMPUTING

Topological quantum computation seeks to exploit the emergent properties of many-particle systems to encode and manipulate quantum information in a manner that is resistant to error. This scheme of quantum computing supports the gate model of quantum computation. Quantum information is stored in states with multiple quasi particles called *anyons*, which have a topological degeneracy and are defined in the next section. The unitary gate operations that are necessary for quantum computation are carried out by performing *braiding* operation on the anyons and then measuring the multiquasipartite states. The fault tolerance of a topological quantum computer arises from the nonlocal encoding of the quasipartite states, which render them immune to errors by local perturbations.

A. Anyons

Two-dimensional systems are qualitatively different [82] from three-dimensional ones. In three-dimensional space, only two symmetries are possible: the time-dependent wave function of bosons is symmetric under exchange of particles while that of fermions is antisymmetric. However, in a two-dimensional case when two particles are interchanged twice in a clockwise manner, their trajectory in space-time involves a nontrivial winding, and the system does not necessarily come back

to the same state. The first realization of this topological difference dates back to the 1980s [83,84] and it leads to a difference in the possible quantum mechanical properties for quantum systems when particles are confined to two dimensions. Suppose we have two identical particles in two dimensions. When one particle is exchanged in a counterclockwise manner with the other, the wave function $\psi(\vec{r}_1, \vec{r}_2)$ can change by an arbitrary phase: $\psi(\vec{r}_1, \vec{r}_2) \rightarrow e^{i\phi}\psi(\vec{r}_1, \vec{r}_2)$. The special cases where $\phi = 0, \pi$ correspond to bosons and fermions, respectively. Particles with other values of ϕ are called *anyons* [85].

B. Non-Abelian Braid Groups

In three-dimensional space, suppose we have N indistinguishable particles and we consider all possible trajectories in the space-time (or four-dimensional worldliness), which take these N particles from initial positions $\vec{r}_1, \vec{r}_2, \ldots, \vec{r}_N$ at time t_0 to final positions $\vec{r}'_1, \vec{r}'_2, \ldots, \vec{r}'_N$ at time t_f. Then the different trajectories fall into topological classes corresponding to the elements of the permutation group S_N, with each element specifying how the initial positions are permuted to obtain the final positions. The way the permutation group acts on the states of the system defines the quantum evolution of such a system. Fermions and bosons correspond to the only two one-dimensional irreducible representations of the permutation group of N identical particles.

In two-dimensional space, the topological classes of the trajectories that take these particles from initial positions $\vec{r}_1, \vec{r}_2, \ldots, \vec{r}_N$ at time t_0 to final positions $\vec{r}'_1, \vec{r}'_2, \ldots, \vec{r}'_N$ at time t_f are in one-to-one correspondence with the elements of the braid group $\mathcal{B}_N$. An element of the braid group can be visualized by considering the trajectories of particles as world lines in $(2 + 1)$-dimensional space-time originating at initial positions and terminating at final positions (Fig. 7a). The multiplication of two elements of the braid group is the successive execution of the corresponding trajectories (i.e., the vertical stacking of the two drawings). As shown in Fig. 7b, the order in which they are multiplied is important because the group is *non-abelian*, which means multiplication is not commutative. Algebraically, the braid group can be represented in terms of elementary braid operations, or generators σ_i, with $1 \leq i \leq N - 1$. σ_i is a counterclockwise exchange of the ith and $(i + 1)$th particles. σ_i^{-1} is therefore a clockwise exchange of the ith and the $(i + 1)$th particles. The σ_i's satisfy the defining relations (Fig. 7c)

$$\begin{aligned} \sigma_i\sigma_j &= \sigma_j\sigma_i \qquad \text{if } |i - j| \geq 2 \\ \sigma_i\sigma_{i+1}\sigma_i &= \sigma_{i+1}\sigma_i\sigma_{i+1} \qquad \text{if } 1 \leq i \leq n - 1 \end{aligned} \tag{12}$$

The richness of the braid group is that it supports quantum computation. To define the quantum evolution of a system, we specify how the braid group acts on the states of the system. An element of the braid group, say σ_1, which exchanges particles 1 and 2, is represented by a $g \times g$ unitary matrix $\rho(\sigma_1)$ acting on these

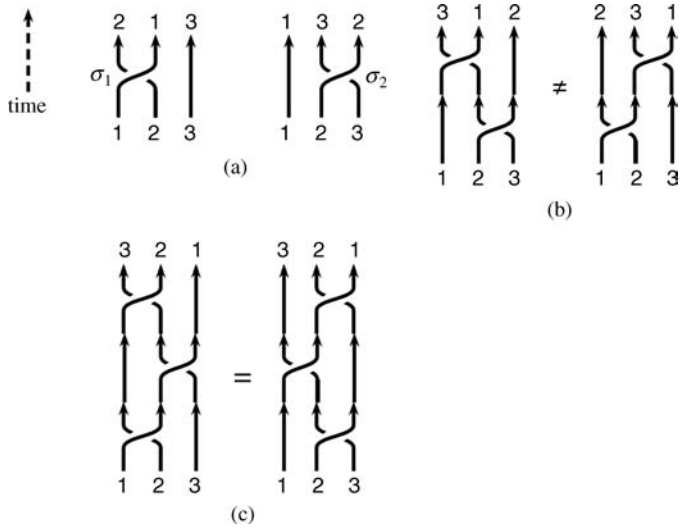

Figure 7. Graphical representation of elements of the braid group. (**a**) The two elementary braid operations σ_1 and σ_2 on three particles. (**b**) Because $\sigma_2\sigma_1 \neq \sigma_1\sigma_2$, the braid group is non-abelian. (**c**) The braid relation.

states,

$$\psi_\alpha \rightarrow [\rho(\sigma_1)]_{\alpha\beta}\psi_\beta \tag{13}$$

Clearly, if $\rho(\sigma_1)$ and $\rho(\sigma_2)$ do not commute, the particles obey *non-abelian braiding statistics*. In this case, braiding quasiparticles will cause nontrivial rotations within the degenerate many-quasiparticle Hilbert space. Furthermore, it will essentially be true at low energies that the only way to make nontrivial unitary operations on this degenerate space is by braiding quasiparticles around each other. Hence, no local perturbation can have nonzero matrix elements within this degenerate space.

C. Topological Phase of Matter

The non-abelian braiding statistics discussed in Section V.B indicates a theoretical possibility, but not any information on the occasions where such braiding statistics may arise in nature. Electrons, photons, and atoms are either fermions or bosons in two-dimensional space. However, if a system of many electrons (or bosons, atoms, etc.) confined to a two-dimensional plane has excitations that are localized disturbances of its quantum mechanical ground state, known as *quasiparticles*, then these quasiparticles can be anyons. When a system has anyonic quasiparticle excitations above its ground state, it is in a *topological phase of matter*.

Topological quantum computation is predicated on the existence in nature of topological phases of matter. Topological phases can be defined as (i) degenerate ground states, (ii) gap to local excitations, (iii) abelian or non-abelian quasiparticle excitations. Because these topological phases occur in many-particle physical systems, field theory techniques are often used to study these states. Hence, the definition of topological phase may be stated more compactly by simply saying that a system is in a topological phase if its low-energy effective field theory is a topological quantum field theory (TQFT), that is, a field theory whose correlation functions are invariant under diffeomorphisms. For a more detailed account of recent development in TQFT and topological materials, see the work of Vala and coworkers (see chapter by Watts et al.).

D. Quantum Computation Using Anyons

The braiding operation $\rho(\sigma_i)$ defined in Eq. (13) can be cascaded to perform quantum gate operation. For example, Georgiev [86] showed that a CNOT gate can be executed on a six-quasiparticle system (for details refer to Ref. [86] or a comprehensive review in Ref. [87]):

$$\rho(\sigma_3^{-1}\sigma_4\sigma_3\sigma_1\sigma_5\sigma_4\sigma_3^{-1}) = \begin{pmatrix} 1 & 0 & 0 & 0 \\ 0 & 1 & 0 & 0 \\ 0 & 0 & 0 & 1 \\ 0 & 0 & 1 & 0 \end{pmatrix} \tag{14}$$

In the construction by Georgiev, quasiparticles 1 and 2 are combined to be qubit 1 via an operation called *fusion*. Similarly, quasiparticles 5 and 6 are combined to be qubit 2. We will not be concerned about the details of fusion in this introduction. Interested readers can refer to Ref. [87], Section II for more information. Apart from CNOT, single-qubit gates are also needed for universal quantum computation. One way to implement those single-qubit gates is to use nontopological operations. More details on this topic can be found in Ref. [88].

VI. ENTANGLEMENT

The concept of *entanglement* can be defined based on a postulate of quantum mechanics. The postulate states that the state space of a composite physical system is the tensor product of the states of the component physical systems. Moreover, if we have systems numbered 1 through n, and the system number i is prepared in the state $|\psi_i\rangle$, then the joint state of the total system is $|\psi\rangle = |\psi_1\rangle \otimes |\psi_2\rangle \otimes \ldots \otimes |\psi_n\rangle$. However, in some cases $|\psi\rangle$ cannot be written in the form of a tensor product of states of individual component systems. For example, the well-known Bell state or EPR pair (named after Einstein, Podolsky, and Rosen for their

initial proposition of this state [89]) $|\psi\rangle = \frac{1}{\sqrt{2}}(|00\rangle + |11\rangle)$ cannot be written in form of $|a\rangle \otimes |b\rangle$. States such as this are called *entangled states*. The opposite case is a *disentangled state*.

In fact, entanglement in a state is a physical property that should be quantified mathematically, which leads to a question of defining a proper expression for calculating entanglement. Various definitions have been proposed to mathematically quantify entanglement (for a detailed review see Refs. [5,90]). One of the most commonly used measurement for pairwise entanglement is *concurrence* $C(\rho)$, where ρ is the density matrix of the state. This definition was proposed by Wootters [91]. The procedure for calculating concurrence is the following (for more examples illustrating how to calculate concurrence in detail, refer to Refs. [5,92,93]):

- Construct the density matrix ρ.
- Construct the flipped density matrix, $\tilde{\rho} = (\sigma_y \otimes \sigma_y)\rho^*(\sigma_y \otimes \sigma_y)$.
- Construct the product matrix $\rho\tilde{\rho}$.
- Find eigenvalues λ_1, λ_2, λ_3, and λ_4 of $\rho\tilde{\rho}$.
- Calculate concurrence from square roots of eigenvalues via

$$C = \max\left(0, \sqrt{\lambda_1} - \sqrt{\lambda_2} - \sqrt{\lambda_3} - \sqrt{\lambda_4}\right) \tag{15}$$

Physically, $C = 0$ means no entanglement in the two-qubit state ρ and $C = 1$ represents maximum entanglement. Therefore, any state ρ with $C(\rho) > 0$ is an entangled state. An entangled state has many surprising properties. For example, if one measures the first qubit of the EPR pair, two possible results are obtained: 0 with probability $1/2$, where postmeasurement the state becomes $|00\rangle$, and 1 with probability $1/2$, where postmeasurement the state becomes $|11\rangle$. Hence, a measurement of the second qubit always gives the same result as that of the first qubit. The measurement outcomes on the two qubits are therefore correlated in some sense. After the initial proposition by EPR, John Bell [94] proved that the measurement correlation in the EPR pair is stronger than could ever exist between classical systems. These results (refer to Ref. [12], Section 2.6 for details) were the first indication that laws of quantum mechanics support computation beyond what is possible in the classical world.

Entanglement has also been used to measure interaction and correlation in quantum systems. In quantum chemistry, the correlation energy is defined as the difference between the Hartree–Fock limit energy and the exact solution of the nonrelativistic Schrödinger equation. Other measures of electron correlation exist, such as the statistical correlation coefficients [95] and, more recently, the Shannon entropy [96]. Electron correlations strongly influence many atomic, molecular, and solid properties. Recovering the correlation energy for large systems remains one

of the most challenging problems in quantum chemistry. We have used the entanglement as a measure of the electron–electron correlation [5,92,93] and show that the configuration interaction (CI) wave function violates the Bell inequality [97]. Entanglement is directly observable via macroscopic observable called entanglement witnesses [98]. Of particular interest is how entanglement plays a role in conical intersections and Landau–Zener tunneling and whether ideas from quantum information such as teleportation can be used to understand spin correlations in molecules [99].

Since the original proposal by DeMille [100], arrays of ultracold polar molecules have been counted among the most promising platforms for the implementation of a quantum computer [101–103]. The qubit of such an array is realized by a single dipolar molecule entangled via its dipole–dipole interaction with the rest of the array's molecules. Polar molecule arrays appear as scalable to a large number of qubits as neutral atom arrays do, but the dipole–dipole interaction furnished by polar molecules offers a faster entanglement, one resembling that mediated by the Coulomb interaction for ions. At the same time, cold and trapped polar molecules exhibit similar coherence times as those encountered for trapped atoms or ions. The first proposed complete scheme for quantum computing with polar molecules was based on an ensemble of ultracold polar molecules trapped in a one-dimensional optical lattice, combined with an inhomogeneous electrostatic field. Such qubits are individually addressable, thanks to the Stark effect, which is different for each qubit in the inhomogeneous electric field. In collaboration with Wei, Friedrich, and Herschbach [93], we have evaluated entanglement of the pendular qubit states for two linear dipoles, characterized by pairwise concurrence, as a function of the molecular dipole moment and rotational constant, strengths of the external field and the dipole–dipole coupling, and ambient temperature. We also evaluated a key frequency shift, $\delta\omega$, produced by the dipole–dipole interaction. Under conditions envisioned for the proposed quantum computers, both the concurrence and $\delta\omega$ become very small for the ground eigenstate. In principle, such weak entanglement can be sufficient for operation of logic gates, provided the resolution is high enough to detect the $\delta\omega$ shift unambiguously. In practice, however, for many candidate polar molecules it appears a challenging task to attain adequate resolution. Overcoming this challenge, small $\delta\omega$ shift, will be a major contribution to implementation of the DeMille proposal. Moreover, it will open the door for designing quantum logical gate: one-qubit gate (such as the rotational X, Y, Z gates and the Hadamard gate) and two-qubit quantum gates (such as the CNOT gate) for molecular dipole arrays. The operation of a quantum gate [104] such as CNOT requires that manipulation of one qubit (target) depends on the state of another qubit (control). This might be characterized by the shift in the frequency for transition between the target qubit states when the control qubit state is changed. The shift must be kept smaller than the differences required to distinguish among addresses of qubit sites. In order to implement the requisite quantum gates, one

might use algorithmic schemes of quantum control theory for molecular quantum gates developed by de Vivie-Riedle and coworkers [105–107], Herschel Rabitz, and others [108–112].

Recent experimental discoveries in various phenomena have provided further evidence of the existence of entanglement in nature. For example, photosynthesis is one of the most common phenomena in nature. Recent experimental results show that long-lived quantum entanglement are present in various photosynthetic complexes [113–115]. One such protein complex, the Fenna–Matthews–Olson (FMO) complex from green sulfur bacteria [116,117], has attracted considerable experimental and theoretical attention due to its intermediate role in energy transport. The FMO complex plays the role of a molecular wire, transferring the excitation energy from the light-harvesting complex (LHC) to the reaction center (RC) [118–120]. Long-lasting quantum beating over a timescale of hundreds of femtoseconds has been observed [121,122]. The theoretical framework for modeling this phenomenon has also been explored intensively by many authors [123–145].

The FMO complex, considered as an assembly of seven chromophores, is a multipartite quantum system. As such, useful information about quantum correlations is obtained by computing the bipartite entanglement across any of the cuts that divide the seven chromophores into two subsystems, seen in Fig. 8. Similarly, if we take the state of any subsystem of the FMO complex, we can compute the entanglement across any cut of the reduced state of that subsystem [128].

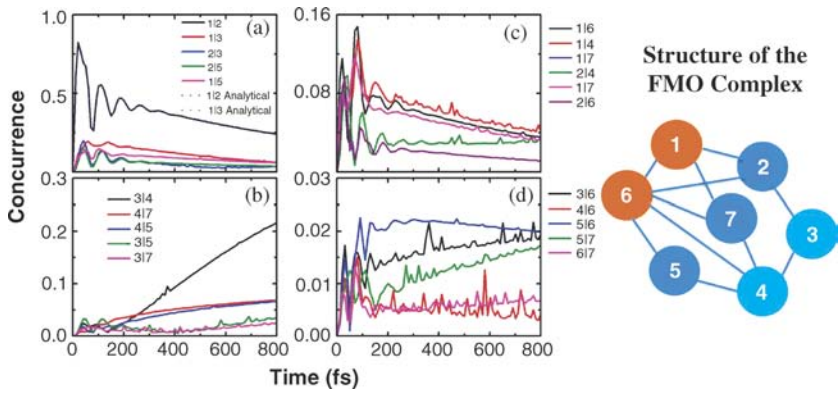

Figure 8. The quantum entanglement evolution for the pairwise entanglement in the FMO complex with the site 1 initially excited. The left panel shows the entanglement with all pairs. Based the amplitude of the concurrence, all pairs had been divided into four groups, from the largest pairs (**a**) to the smallest pairs (**d**). The solid line indicates the entanglement computed via the convex roof approach [147], while the dotted line shows the evolution calculated through the concurrence method. The right panel is the geometry structure of the FMO complex.

Pairwise entanglement plays the dominant entanglement role in the FMO complex. Because of the saturation of the monogamy bounds, the entanglement of any chromophore with any subset of the other chromophores is completely determined by the set of pairwise entanglements. For the simulations in which site 1 is initially excited, the dominant pair is sites 1 and 2, while in the cases where 6 is initially excited sites 5 and 6 are most entangled. This indicates that entanglement is dominant in the early stages of exciton transport, when the exciton is initially delocalized away from the injection site. In addition, we observe that the entanglement mainly happens among the sites involved in the pathway. For the site 1 initially excited case, the entanglement of sites 5, 6, and 7 is relatively small compared with the domain pairs.

Although the final state is the same for both initial conditions, the role of sites 3 and 4 during the time evolution is different. For the initial condition where site 1 is excited, the entanglement is transferred to site 3 and then from site 3 to site 4. While for the site 6 initially excited case, sites 4 and 5 first become entangled with site 6 and then sites 3 and 4 become entangled. This is due to the fact that site 3 has strong coupling with sites 1 and 2, while site 4 is coupled more strongly to sites 5, 6, and 7. The initial condition plays an important role in the entanglement evolution, the entanglement decays faster for the cases where site 6 is initially excited compared with cases where the site 1 is initially excited. Increasing the temperature unsurprisingly reduces the amplitude of the entanglement and also decreases the time for the system to go to thermal equilibrium. Recently [146], using the same formalism, we have calculated the pairwise entanglement for the LH2 complex, as seen in Fig. 9.

Apart from photosynthesis, other intriguing possibilities that living systems may use nontrivial quantum effects to optimize some tasks have been raised, such as natural selection [148] and magnetoreception in birds [149]. In particular, *magnetoreception* refers to the ability to sense characteristics of the surrounding magnetic field. There are several mechanisms by which this sense may operate [150]. In certain species, the evidence supports a mechanism called *radical pair* (RP). This process involves the quantum evolution of a spatially separated pair of electron spins [151,152]. The basic idea of the RP model is that there are molecular structures in the bird's eye that can each absorb an optical photon and give rise to a spatially separated electron pair in a singlet spin state. Because of the different local environments of the two electron spins, a singlet–triplet evolution occurs. This evolution depends on the inclination of the molecule with respect to Earth's magnetic field. Recombination occurs from either the singlet or triplet state, leading to different chemical products. The concentration of these products constitutes a chemical signal correlated to Earth's field orientation. Such a model is supported by several results from the field of spin chemistry [153–156]. An artificial chemical compass operating according to this principle has been demonstrated experimentally [157], and the presence of entanglement has been examined by a theoretical study [158].

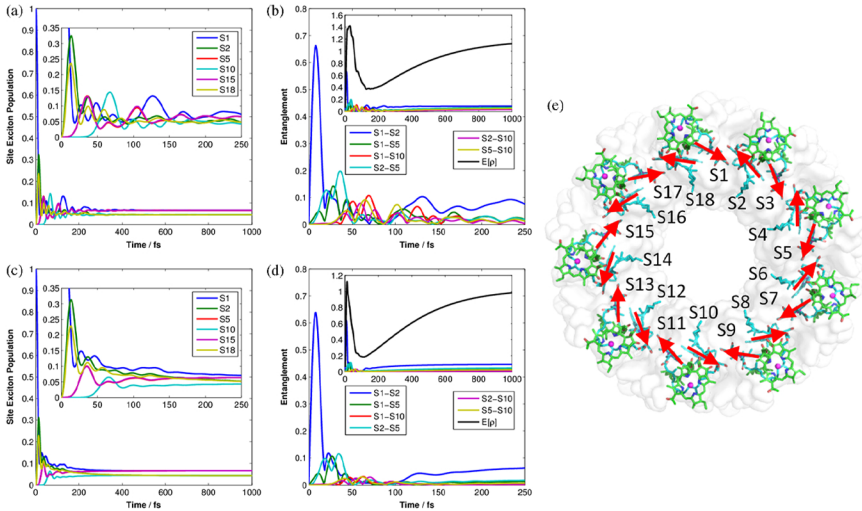

Figure 9. (**a**) The excitation population dynamics of LH2 B850 18 sites at 77 K. (**b**) The concurrence and global entanglement (black line in the inset) in the 18 sites at 77 K. (**c**) The excitation population dynamics of LH2 B850 18 sites at 300 K. (**d**) The concurrence and global entanglement (black line in the inset) in the 18 sites at 300 K. (**e**) Top view (from cytoplasmic to periplasmic side) of 2.0 Å resolution LH2 structure of purple bacteria (*Rhodopseudomonas acidophila*). The 9 B800 and 18 B850 bacteriochlorophylls (BChls) are shown in green and cyan, respectively. The red arrows represent the transition dipoles of B850 BCHls Q_Y excitation. Top view (from cytoplasmic to periplasmic side) of 2.0 Å resolution LH2 structure of purple bacteria. The 9 B800 and 18 B850 bacteriochlorophylls (BChls) are shown in green and cyan, respectively. The red arrows represent the transition dipoles of B850 BCHls Q_Y excitation [146].

Not only is entanglement found in nature, but it also plays a central role in the internal working of a quantum computer. Consider a system of two qubits 1 and 2. Initially, qubit 1 is in the state $|\psi_1\rangle = |+\rangle = \frac{1}{\sqrt{2}}(|0\rangle + |1\rangle)$ and qubit 2 is in the state $|\psi_2\rangle = |0\rangle$. Hence, the initial state of the system can be written as $|\Psi_0\rangle = |\psi_1\rangle \otimes |\psi_2\rangle = \frac{1}{\sqrt{2}}(|00\rangle + |10\rangle)$. Now apply a CNOT on qubits 1 and 2 with qubit 1 as the control and qubit 2 as the target. By definition of CNOT gate in Section I.A, the resulting state is $\frac{1}{\sqrt{2}}(|00\rangle + |11\rangle)$, which is the EPR pair. Note that the two qubits are initially disentangled. It is due to the CNOT operation that the two qubits are in an entangled state. Mathematically U_{CNOT} cannot be represented as $A \otimes B$, because if it could, $(A \otimes B)(|\psi_1\rangle \otimes |\psi_2\rangle) = (A|\psi_1\rangle \otimes B|\psi_2\rangle)$ would still yield a disentangled state.

CNOT gate is indispensable for any set of universal quantum gates. Therefore, if a particular computation process involves n qubits that are initially disentangled, most likely all the n qubits need to be entangled at some point of the computation. This poses a great challenge for experimentalists because in order to keep a large number of qubits entangled for an extended period of time, a major issue needs to be resolved—decoherence.

VII. DECOHERENCE

So far in our discussion of qubits, gates, and algorithms we assume the ideal situation where the quantum computer is perfectly isolated when performing computation. However, in reality this is not feasible because there is always interaction between the quantum computer and its environment, and if one would like to read any information from the final state of the quantum computer, the system has to be open to measurements at least at that point. Therefore, a quantum computer is in fact constantly subject to environmental noise, which corrupts its desired evolution. Such unwanted interaction between the quantum computer and its environment is called *decoherence*, or *quantum noise*.

Decoherence has been a main obstacle to building a quantum computing device. Over the years, various ways of suppressing quantum decoherence have been explored [159]. The three main error correction strategies for counteracting the errors induced by the coupling with the environment include the following (see chapter by Lidar):

- Quantum error correction codes (QECCs), which uses redundancy and an active measurement and recovery scheme to correct errors that occur during a computation [160–164]
- Decoherence-free subspaces (DFSs) and noiseless subsystems, which rely on symmetric system–bath interactions to end encodings that are immune to decoherence effects [165–170]

- Dynamical decoupling, or "bang-bang" (BB) operations, which are strong and fast pulses that suppress errors by averaging them away [171–175]

Of these error correction techniques, QECCs require at least a five physical qubit to one logical qubit encoding [163] (neglecting ancillas required for fault-tolerant recovery) in order to correct a general single-qubit error [162]. DFSs also require extra qubits and are most effective for collective errors, or errors where multiple qubits are coupled to the same bath mode [170]. The minimal encoding for a single qubit undergoing collective decoherence is three physical qubits to one logical qubit [168]. The BB control method requires a complete set of pulses to be implemented within the correlation time of the bath [171]. However, it does not necessarily require extra qubits.

Although the ambitious technological quest for a quantum computer has faced various challenges, as of now no fundamental physical principle has been found to prevent a scalable quantum computer from being built. Therefore, if we keep this prospect, one day we will be able to maintain entanglement and overcome decoherence to a degree such that scalable quantum computers become reality.

VIII. MAJOR CHALLENGES AND OPPORTUNITIES

Many of the researchers in the quantum information field have recognized quantum chemistry as one of the early applications of quantum computing devices. This recognition is reflected in the document "A Federal Vision for Quantum Information Science," published by the Office of Science and Technology Policy (OSTP) of the White House. As mentioned earlier, the development and use of quantum computers for chemical applications has potential for revolutionary impact on the way computing is done in the future. Major challenges and opportunities are abundant; examples include developing and implementing quantum algorithms for solving chemical problems thought to be intractable for classical computers. To perform such quantum calculations, it will be necessary to overcome many challenges in experimental quantum simulation. New methods to suppress errors due to faulty controls and noisy environments will be required. These new techniques would become part of a quantum compiler that translates complex chemical problems into quantum algorithms. Other challenges include the role of quantum entanglement, coherence, and superposition in photosynthesis and complex chemical reactions.

Many exciting opportunities for science and innovation can be found in this new area of quantum information for chemistry including topological quantum computing (see chapter by Watts et al.), improving classical quantum chemistry methods (see chapter by Kinder et al.), quantum error corrections (see chapter by Lidar), quantum annealing with D-Wave machine [176], quantum algorithms for solving linear systems of equations, and entanglement in complex biological systems (see chapter by Mazziotti and Skochdopole). With its 128 qubits, the

D-Wave computer at USC (the DW-1) is the largest quantum information processor built to date. This computer will grow to 512 qubits (the chip currently being calibrated and tested by D-Wave Inc. (D. A. Lidar, private communication, USC, 2012)), at which point we may be on the cusp of demonstrating, for the first time in history, a quantum speedup over classical computation. Various applications of DW-1 in chemistry include, for example, the applications in cheminformatics (both in solar materials and in drug design) and in lattice protein folding, and the solution of the Poisson equation and its applications in several fields. While the DW-1 is not a universal quantum computer, it is designed to solve an important and broad class of optimization problems—essentially any problem that can be mapped to the NP-hard problem of finding the ground state of a general planar Ising model in a magnetic field.

This chapter focused mainly on the theoretical aspects of quantum information and computation for quantum chemistry and represents a partial overview of the ongoing research in this field. However, a number of experimental groups are working to explore quantum information and computation in chemistry: using ion trap (see chapter by Merrill and Brown) [177], NMR (see chapter by Criger et al.) [178–182], trapped molecules in optical lattice (see chapter by Côté) [183], molecular states (see chapter by Gollub et al.) [184,185], and optical quantum computing platforms (see chapter by Ma et al.) [186,187], to name just a few. For example, Brown and coworkers [177] proposed a method for laser cooling of the AlH^+ and BH molecules. One challenge of laser cooling molecules is the accurate determination of spectral lines to 10^{-5} cm^{-1}. In their work, the authors show that the lines can be accurately determined using quantum logic spectroscopy and sympathetic heating spectroscopy techniques, which were derived from quantum information experiments. Also, Dorner and coworkers [188] perform the simplest double-slit experiment to understand the role of interference and entanglement in the double photoionization of H_2 molecule. Moreover, many more areas of overlap have not been reviewed in detail here, notably coherent quantum control of atoms and molecules. However, we hope this chapter provides a useful introduction to the current research directions in quantum information and computation for chemistry.

Finally, I would like to end this chapter by quoting Jonathan Dowling [189]: "We are currently in the midst of a second quantum revolution. The first one gave us new rules that govern physical reality. The second one will take these rules and use them to develop new technologies. Today there is a large ongoing international effort to build a quantum computer in a wide range of different physical systems. Suppose we build one, can chemistry benefit from such a computer? The answer is a resounding YES!"

Acknowledgments

I would like thank Birgitta Whaley for her critical reading of this chapter and my students Yudong Cao, Anmer Daskin, Jing Zhu, Yeh Shuhao, Qi Wei, Qing Xu,

and Ross Hoehn for their major contributions to the materials discussed in this chapter. Also, I benefited from collaborating and discussing different aspects of this chapter with my colleagues: Alan Aspuru-Guzik, Daniel Lidar, Ken Brown, Peter Love, V. Ara Apkarian, Anargyros Papageorgiou, Bretislav Friedrich, Uri Peskin, Gehad Sadiek, and Dudley Herschbach.

This work is supported by NSF Center for Quantum Information for Chemistry (QIQC), http://web.ics.purdue.edu/ kais/qc/ (award number CHE-1037992).

REFERENCES

1. M. Sarovar, A. Ishizaki, G. R. Fleming, and K. B. Whaley, *Nat. Phys.* **6**, 462 (2010).
2. K. B. Whaley, *Nat. Phys.* **8**, 10 (2012).
3. I. Kassal, J. D. Whitfield, A. Perdomo-Ortiz, M. Yung, and A. Aspuru-Guzik, *Annu. Rev. Phys. Chem.* **62**, 185 (2011).
4. W. J. Kuo and D. A. Lidar, *Phys. Rev. A* **84**, 042329 (2011).
5. S. Kais, in *Reduced-Density-Matrix Mechanics: With Application to Many-Electron Atoms and Molecules, Advances in Chemical Physics*, Vol. 134, D. A. Mazziotti, ed., Wiley-Interscience, 2007, p. 493.
6. S. Lloyd, *Science* **319**, 1209 (2008).
7. J. Elbaz, O. Lioubashevski, F. Wang, F. Remacle, R. D. Levine, and I. Willner. *Nat. Nanotechnol.* **5**, 417–422 (2011).
8. R. P. Feynmann, *Int. J. Theor. Phys.* **21**(6–7), 467–488 (2008).
9. D. Deutsch, *Proc. R. Soc. Lond.* **400**, 97–117 (1985).
10. P. Benioff, *J. Stat. Phys.* **29**, 515–546 (1982).
11. C. H. Bennett and G. Brassard, *Proceedings of IEEE International Conference on Computers Systems and Signal Processing*, 1984, pp. 175–179.
12. M. A. Nielsen and I. L. Chuang, *Quantum Computation and Quantum Information*, Cambridge University Press, Cambridge, UK, 2000.
13. P. W. Shor, in *Proceedings of the 35th Annual Symposium on Foundations of Computer Science*, S. Goldwasser, ed., IEEE Computer Society Press, New York, 1994, pp. 124–134.
14. S. Lloyd, *Science* **273**, 1073–1078 (1996).
15. D. Abrams and S. Lloyd, *Phys. Rev. Lett.* **83**(24), 5162–5165 (1999).
16. D. Abrams and S. Lloyd, *Phys. Rev. Lett.* **79**(13), 2586–2589 (1997).
17. A. Papageorgiou, I. Petras, J. F. Traub, and C. Zhang, *Mathematics of Computation* **82**, 2293–2304 (2013).
18. A. Papageorgiou and C. Zhang, arXiv:1005.1318v3 (2010).
19. H. Wang, S. Kais, A. Aspuru-Guzik, and M. R. Hoffmann, *Phys. Chem. Chem. Phys.* **10**, 5388–5393 (2008).
20. A. Aspuru-Guzik, A. D. Dutoi, P. J. Love, and M. Head-Gordon, *Science* **379**(5741), 1704–1707 (2005).
21. D. Lidar and H. Wang, *Phys. Rev. E* **59**, 2429 (1999).
22. H. Wang, S. Ashhab, and F. Nori, *Phys. Rev. A* **85**, 062304 (2012).
23. J. Q. You and F. Nori, *Nature* **474**, 589 (2011).

24. J. Q. You and F. Nori, *Phys. Today* **58**(11), 42–47 (2005).
25. I. Buluta and F. Nori, *Science* **326**, 108 (2009).
26. J. P. Dowling, *Nature* **439**, 919 (2006).
27. L. Veis and J. Pittner, *J. Chem. Phys.* **133**, 194106 (2010).
28. L. Veis, J. Visnak, T. Fleig, S. Knecht, T. Saue, L. Visscher, and J. Pittner, arXiv:1111.3490v1 (2011).
29. A. W. Harrow, A. Hassidim, and S. Lloyd, *Phys. Rev. Lett.* **15**, 150502 (2009).
30. A. Klappenecker and M. Roetteler, arXiv:quant-ph/0111038 (2001).
31. P. A. M. Dirac, *Proc. Roy. Soc.* **123**, 714 (1929).
32. S. Aaronson, *Nat. Phys.* **5**, 707 (2009).
33. N. Schuch and F. Verstraete, *Nat. Phys.* **5**, 732 (2009).
34. A. Szabo and N. S. Ostlund, *Modern Quantum Chemistry—Introduction to Advanced Electronic Structure Theory*, Dover Publications Inc., Mineola, NY, 1982.
35. R. G. Parr and W. Yang, *Density-Functional Theory of Atoms and Molecules*, Oxford Science Publications, New York, 1989.
36. D. A. Mazziotti, *Adv. Chem. Phys.* **134**, 1 (2007).
37. I. Iachello and R. D. Levine, *Algebraic Theory of Molecules*, Oxford Univesity Press, 1995.
38. M. P. Nightingale and C. J. Umrigar, *Quantum Monte Carlo Methods in Physics and Chemistry*, *NATO Science Series*, Vol. 525, Springer, 1998.
39. D. R. Herschbach, J. Avery, and O. Goscinski, *Dimensional Scaling in Chemical Physics*, Kluwer Academic Publishers, Dordrecht, The Netherlands, 1993.
40. H. Dachsel, R. J. Harrison, and D. A. Dixon, *J. Phys. Chem. A* **103**, 152–155 (1999).
41. D. P. DiVincenzo, arXiv:quant–ph/0002077 (2000).
42. T. D. Ladd, F. Jelezko, R. Laflamme, Y. Nakamura, C. Monroe, and J. L. O'Brien, *Nature* **464**(4), 45 (2010).
43. R. L. de Visser and M. Blaauboer, *Phys. Rev. Lett.* **96**, 246801 (2006).
44. P. Jian-Wei, B. Dik, D. Matthew, W. Harald, and A. Zeilinge, *Nature* **403**, 515 (2000).
45. P. Chen, C. Piermarocchi, and L. J. Sham, *Phys. Rev. Lett.* **87**, 067401 (2001).
46. F. de Pasquale, G. Giorgi, and S. Paganelli, *Phys. Rev. Lett.* **93**, 12052 (2004).
47. J. H. Reina and N. F. Johnson, *Phys. Rev. A* **63**, 012303 (2000).
48. D. Bouwmeester, J. Pan, K. Mattle, M. Eibl, H. Weinfurter, and A. Zeilinger, *Nature* **390**, 575 (1997).
49. C. W. J. Beenakker and M. Kindermann, *Phys. Rev. Lett.* **95**, 056801 (2004).
50. M. D. Barrett, J. Chiaverinl, and T. Schaetz, et al., *Nature* **429**, 737 (2004).
51. M. Riebe, et al., *Nature* **429**, 734 (2004).
52. H. Wang and S. Kais, *Chem. Phys. Lett.* **421**, 338 (2006).
53. C. H. Bennett, G. Brassard, C. Crepeau, R. Jozsa, A. Peres, and W. Wootters, *Phys. Rev. Lett.* **70**, 1895 (1993).
54. C. P. Williams. *Explorations in Quantum Computing*, 2nd ed., Springer, 2011, p. 483.
55. R. Ursin, T. Jennewein, M. Aspelmeyer, R. Kaltenbaek, M. Lindenthal, P. Walther, and A. Zeilinge, *Nature* **430**, 849 (2004).
56. R. Ursin, F. Tiefenbacher, T. Schmitt-Manderbach, et al., *Nat. Phys.* **3**, 481 (2007).
57. H. Wang and S. Kais, in *Handbook of Nanophysics*, K. Sattler, ed., Taylor & Francis, 2012.

58. B. P. Lanyon, J. D. Whitfield, G. G. Gillet, M.l E. Goggin, M. P. Almeida, I. Kassal, J. D. Biamonte, M. Mohseni, B. J. Powell, M. Barbieri, A. Aspuru-Guzik, and A. G. White, *Nat. Chem.* **2**, 106–111 (2009).
59. L. M. K. Vandersypen, M. Steffen, G. Breyta, C. S. Yannoni, M. H. Sherwood, and I. L. Chuang, *Nature* **413**, 883–887 (2001).
60. M. Mosca, Quantum computer algorithms, Ph.D. thesis, University of Oxford, 1999.
61. A. Daskin and S. Kais, *J. Chem. Phys.* **134**, 144112 (2011).
62. A. Daskin and S. Kais, *Mol. Phys.* **109**(5), 761–772 (2011).
63. E. Farhi, J. Goldstone, S. Gutmann, and M. l Sisper, arXiv:quant-ph/0001106v1 (2000).
64. D. Aharonov, W. van Dam, J. Kempe, Z. Landau, S. Lloyd, and O. Regev, *SIAM J. Comput.* **37**(1), 166–194 (2007).
65. W. van Dam, M. Mosca, and U. Vazirani, *Proceedings of the 42nd Symposium on Foundations of Computer Science*, 2001, pp. 279–287.
66. E. Farhi, J. Goldstone, S. Gutmann, J. Lapan, A. Lundgren, and D. Preda, *Science* **292**(5516), 472–476 (2001).
67. J. Kempe, A. Kitaev, and O. Regev, *SIAM J. Comput.* **35**, 1070 (2006).
68. J. D. Biamonte and P. J. Love, *Phys. Rev. A* **78**, 012352 (2008).
69. S. Bravyi, D. P. DiVincenzo, R. I. Oliveira, and B. M. Terhal, *Quant. Inf. Comput.* **8**(5), 0361–0385 (2008).
70. A. Kitaev, A. Shen, and M. Vyalyi, *Classical and Quantum Computation: Graduate Studies in Mathematics*, Vol. 47, American Mathematical Society, Providence, RI, 2002.
71. R. Harris, A. J. Berkley, M. W. Johnson, P. Bunyk, S. Govorkov, M. C. Thom, S. Uchaikin, A. B. Wilson, J. Chung, E. Holtham, J. D. Biamonte, A. Yu. Smirnov, M. H. S. Amin, and A. M. van den Brink, *Phys. Rev. Lett.* **98**, 177001 (2007).
72. R. Harris, M. W. Johnson, T. Lanting, A. J. Berkley, J. Johansson, P. Bunyk, E. Tolkacheva, E. Ladizinsky, N. Ladizinsky, T. Oh, F. Cioata, I. Perminov, P. Spear, C. Enderud, C. Rich, S. Uchaikin, M. C. Thom, E. M. Chapple, J. Wang, B. Wilson, M. H. S. Amin, N. Dickson, K. Karimi, B. Macready, C. J. S. Truncik, and G. Rose, *Phys. Rev. B* **82**, 024511 (2010).
73. T. Kato, *J. Phys. Soc. Jap.* **5**, 435–439 (1951).
74. A. Messiah, *Quantum Mechanics*, Wiley, New York, 1958.
75. B. Reichardt, *Proceedings of the 36th Symposium on Theory of Computing*, 2004, pp. 502–510.
76. R. Oliveira and B. Terhal, *Quant. Inf. and Comp.* **8**, 900–924 (2008).
77. J. D. Biamonte, *Phys. Rev. A* **77**(5), 052331 (2008).
78. J. D. Biamonte and P. J. Love, *Phys. Rev. A* **8**(1), 012352 (2008).
79. S. Jordan and E. Farhi, *Phys. Rev. A* **77**, 062329 (2008).
80. M. Wolf, *Nat. Phys.*, **4**, 834–835 (2008).
81. J. Kempe, A. Kitaev, and O. Regev, *SIAM J. Comput.* **35**(5), 1070–1097 (2006).
82. A. Stern, *Ann. Phys.* **323**, 204–249 (2008).
83. J. M. Leinaas and J. Myrheim, *Nuovo Climento Soc. Ital. Fis. B* **37**, 1 (1977).
84. F. Wilczek, *Phys. Rev. Lett.* **48**, 1144 (1982).
85. F. Wilczek, *Fractional Statistics and Anyon Superconductivity*, World Scientific, Singapore, 1990.
86. L. S. Georgiev, *Phys. Rev. B* **74**, 235112 (2006).

87. C. Nayak, S. H. Simon, A. Stern, M. Freedman, and S. Das Sarma, *Rev. Mod. Phys.* **80**, 1083 (2008).
88. S. Bravyi, *Phys. Rev. A* **73**, 042313 (2006).
89. A. Einstein, B. Podolsky, and N. Rosen, *Phys. Rev.* **47**, 777–780 (1935).
90. L Amico, R. Fazio, A. Osterioh, and V. Vedral, *Rev. Mod. Phys.* **80**, 518 (2003).
91. W. K. Wootters, *Phys. Rev. Lett.* **80**, 2245–2248 (1998).
92. Z. Huang and S. Kais, *Chem. Phys. Lett.* **413**, 1–5 (2005).
93. Q. Wei, S. Kais, B. Fredrich, and D. Herschbach, *J. Chem. Phys.* **134**, 124107 (2011).
94. J. S. Bell, *Physics* **1**(3), 195–200 (1964).
95. W. Kutzelnigg, G. Del Re, and G. Berthier, *Phys. Rev.* **172**, 49 (1968).
96. Q. Shi and S. Kais, *J. Chem. Phys.* **121**, 5611 (2004).
97. H. Wang and S. Kais, *Israel J. Chem.* **47**, 59–65 (2007).
98. L. A. Wu, S. Bandyopadhyay, M. S. Sarandy, and D. A. Lidar, *Phys. Rev. A* **72**, 032309 (2005).
99. H. Wang and S. Kais, in *Handbook of Nanophysics*, K. Sattler, ed., Springer, 2011.
100. D. DeMille, *Phys. Rev. Lett.* **88**, 067901 (2002).
101. R. V. Krems, W. C. Stwalley, and B. Friedrich, *Cold Molecules: Theory, Experiment, Applications*, Taylor & Francis, 2009.
102. B. Friedrich and J. M. Doyle, *ChemPhysChem* **10**, 604 (2009).
103. S. F. Yelin, K. Kirby, and R. Cote, *Phys. Rev. A* **74**, 050301(R) (2006).
104. J. Z. Jones, *PhysChemComm* **11**, 1 (2001).
105. B. M. R. Schneider, C. Gollub, K. L. Kompa, and R. de Vivie-Riedle, *Chem. Phys.* **338**, 291 (2007).
106. B. M. R. Korff, U. Troppmann, K. L. Kompa, and R. de Vivie-Riedle, *J. Chem. Phys.* **123**, 244509 (2005).
107. U. Troppmann, C. M. Tesch, and R. de Vivie-Riedle, *Chem. Phys. Lett.* **378**, 273 (2003).
108. M. P. A. Branderhorst, et al., *Science* **638**, 320 (2008).
109. H. Rabitz, *Science* **314**, 264 (2006).
110. W. Warren, H. Rabitz, and M. Dahleh, *Science* **259**, 1581 (1993).
111. D. Babikov, *J. Chem. Phys.* **121**, 7577 (2004).
112. D. Sugny, L. Bomble, T. Ribeyre, O. Dulieu, and M. Desouter-Lecomte, *Phys. Rev. A* **80**, 042325 (2009).
113. D. L. Andrews and A. A. Demidov, *Resonance Energy Transfer*, Wiley, 1999.
114. G. D. Scholes, *J. Phys. Chem. Lett.* **1**(1), 2–8 (2010).
115. G. D. Scholes, *Nat. Phys.* **6**, 402–403 (2010).
116. R. E. Fenna and B. W. Matthews, *Nature* **258**, 573–577 (1975).
117. R. E. Fenna, B. W. Matthews, J. M. Olson, and E. K. Shaw, *J. Mol. Biol.* **84**, 231–234 (1974).
118. Y. F. Li, W. L. Zhou, R. E. Blankenship, and J. P. Allen, *J. Mol. Biol.* **271**, 456–471 (1997).
119. A. Camara-Artigas, R. E. Blankenship, and J. P. Allen, *Photosynth Res.* **75**, 49–55 (2003).
120. Y. C. Cheng and G. R. Fleming, *Annu. Rev. Phys. Chem.* **60**, 241–262 (2009).
121. G. S. Engel, T. R. Calhoun, E. L. Read, T. K. Ahn, T. Mancal, Y.-C. Cheng, R. E. Blankenship, and G. R. Fleming, *Nature* **446**, 782–786 (2007).
122. G. Panitchayangkoon, D. Hayes, K. A. Fransted, J. R. Caram, E. Harel, J. Wen, R. E. Blankenship, and G. S. Engel, *Proc. Natl. Acad. Sci. USA* **107**, 12766–12770 (2010).

123. M. Mohseni, P. Rebentrost, S. Lloyd, and A. Aspuru-Guzik, *J. Chem. Phys.* **129**, 174106 (2008).
124. P. Rebentrost, M. Mohseni, I. Kassal, S. Lloyd, and A. Aspuru-Guzik, *New J. Phys.* **11**, 033003 (2009).
125. P. Rebentrost, M. Mohseni, and A. Aspuru-Guzik, *J. Phys. Chem. B* **113**, 9942–9947 (2009).
126. A. Ishizaki and G. R. Fleming, *J. Chem. Phys.* **130**, 234111 (2009).
127. A. Ishizaki and G. R. Fleming, *Proc. Natl. Acad. Sci. USA* **106**, 17255–17260 (2009).
128. J. Zhu, S. Kais, P. Rebentrost, and A. Aspuru-Guzik, *J. Phys. Chem. B* **115**, 1531–1537 (2011).
129. Q. Shi, L. P. Chen, G. J. Nan, X. R. Xu, and Y. J. Yan, *J. Chem. Phys.* **130**, 084105 (2009).
130. T. Kramer, C. Kreisbeck, M. Rodriguez, and B. Hein, *American Physical Society March Meeting*, 2011.
131. T. C. Berkelbach, T. E. Markland, and D. R. Reichman, arXiv:1111.5026v1 (2011).
132. J. Prior, A. W. Chin, S. F. Huelga, and M. B. Plenio, *Phys. Rev. Lett.* **105**, 050404 (2010).
133. P. Huo and D. F. Coker, *J. Chem. Phys.* **133**, 184108 (2010).
134. J. Moix, J. Wu, P. Huo, D. Coker, and J. Cao, *J. Phys. Chem. Lett.* **2**, 3045–3052 (2011).
135. N. Skochdopole and D. A. Otti, *J. Phys. Chem. Lett.* **2**(23), 2989–2993 (2011).
136. D. A. Mazziotti, arXiv: 1112.5863v1 (2011).
137. P. Nalbach, D. Braun, and M. Thorwart, *Phys. Rev. E* **84**, 041926 (2011).
138. A. Shabani, M. Mohseni, H. Rabitz, and S. Lloyd, arXiv:1103.3823v3 (2011).
139. M. Mohseni, A. Shabani, S. Lloyd, and H. Rabitz, arXiv:1104.4812v1 (2011).
140. S. Lloyd, M. Mohseni, A. Shabani, and H. Rabitz, arXiv:1111.4982v1 (2011).
141. J. H. Kim and J. S. Cao, *J. Phys. Chem. B* **114**, 16189–16197 (2010).
142. J. L. Wu, F. Liu, Y. Shen, J. S. Cao, and R. J. Silbey, *New J. Phys.* **12**, 105012 (2010).
143. S. M. Vlaming and R. J. Silbey, arXiv:1111.3627v1 (2011).
144. N. Renaud, M. A. Ratner, and V. Mujica, *J. Chem. Phys.* **135**, 075102 (2011).
145. D. Abramavicius and S. Mukamel, *J. Chem. Phys.* **133**, 064510 (2010).
146. S. Yeh, J. Zhu, and S. Kais, *J. Chem. Phys.* **137**, 084110 (2012).
147. J. Zhu, S. Kais, A. Aspuru-Guzik, S. Rodriques, B. Brock, and P. Love, *J. Chem. Phys.* **137**, 074112 (2012).
148. S. Lloyd, *Nat. Phys.* **5**, 164–166 (2009).
149. E. M. Gauger, E. Rieper, J. L. Morton, S. C. Benjamin, and V. Vedral, *Phys. Rev. Lett.* **106**, 040503 (2011).
150. S. Johnsen and K. J. Lohmann, *Phys. Today* **61**(3), 29–35 (2008).
151. T. Ritz, S. Adem, and K. Schulten, *Biophys. J.* **78**, 707–718 (2000).
152. T. Ritz, P. Thalau, J. B. Phillips, R. Wiltschko, and W. Wiltschko, *Phys. Rev. Lett.* **106**, 040503 (2011).
153. C. R. Timmel and K. B. Henbest, *Philos. Trans. R. Soc. A* **362**, 2573 (2004).
154. T. Miura, K. Maeda, and T. Arai, *J. Phys. Chem.* **110**, 4151 (2006).
155. C. T. Rodgers, *Pure Appl. Chem.* **81**, 19–43 (2009).
156. C. T. Rodgers and P. J. Hore, *Proc. Natl. Acad. Sci. USA* **106**, 353–360 (2009).
157. K. Maeda, K. B. Henbest, F. Cintolesi, I. Kuprov, C. T. Rodgers, P. A. Liddell, D. Gust, C. R. Timmel, and P. J. Hore, *Nature* **453**, 387 (2008).
158. J. Cai, G. G. Guerreschi, and H. J. Briegel, *Phys. Rev. Lett.* **104**, 220502 (2010).
159. M. S. Byrd and D. A. Lidar, *J. Mod. Opt.* **50**, 1285 (2003).

160. P. W. Shor, *Phys. Rev. A* **52**, 2493–2496 (1995).
161. A. M. Steane, *Phys. Rev. Lett.* **77**, 793–797 (1996).
162. D. Gottesman, *Phys. Rev. A* **54**, 1862 (1996).
163. E. Knill and R. Laflamme, *Phys. Rev. A* **55**, 900–911 (1997).
164. A. M. Steane, *Introduction to Quantum Computation and Information*, World Scientific, Singapore, 1999.
165. P. Zanardi and M. Rasetti, *Phys. Rev. Lett.* **79**, 3306–3309 (1997).
166. L. Duan and G. C. Guo, *Phys. Rev. A* **57**, 737 (1998).
167. D. A. Lidar, I. L. Chuang, and K. B. Whaley, *Phys. Rev. Lett.* **81**, 2594 (1998).
168. E. Knill, R. Laflamme, and L. Viola, *Phys. Rev. Lett.* **84**, 2525 (2000).
169. J. Kempe, D. Bacon Dave, D. A. Lidar, and B. K. Whaley, *Phys. Rev. A* **63**, 042307 (2001).
170. D. A. Lidar, D. Bacon, J. Kempe, and K. B. Whaley, *Phys. Rev. A* **63**, 022306 (2001).
171. L. Viola and S. Lloyd, *Phys. Rev. A* **58**, 2733 (1998).
172. L.-M. Duan and G.-C. Guo, *Phys. Lett. A* **261**, 139 (1999).
173. L. Viola, E. Knill, and S. Lloyd, *Phys. Rev. Lett.* **82**, 2417 (1999).
174. P. Zanardi, *Phys. Lett. A* **77**, 258 (1999).
175. D. Vitali and P. Tombesi, *Phys. Lett. A* **59**, 4178–4186 (1999).
176. M. W. Johnson et al., *Nature* **473**, 194 (2011).
177. J. H. V. Nguyen, C. R. Viteri, E. G. Hohenstein, C. D. Sherrill, K. R Brown, and B. Odoml, *New J. Phys.* **13**, 063023 (2011).
178. L. M. K. Vandersypen and I. L. Chuang, *Rev. Mod. Phys.* **76**, 1037 (2005).
179. C. Negrevergne, T. S. Mahesh, C. A. Ryan, M. Ditty, F. Cyr-Racine, W. Power, N. Boulant, T. Havel, D. G. Cory, and R. Laflamme, *Phys. Rev. Lett.* **96**, 170501 (2006).
180. Y. Zhang, C. A. Ryan, R. Laflamme, and J. Baugh, *Phys. Rev. Lett.* **107**, 170503 (2011).
181. G. Brassad, I. Chuang, S. Lloyd, and C. Monroe, *Proc. Natl. Acad. Sci. USA* **95**, 11032 (1998).
182. D. Lu, et al., *Phys. Rev. Lett.* **107**, 020501 (2011).
183. E. S. Shuman, J. F. Barry, and D. DeMille, *Nature* **467**, 820 (2010).
184. J. Vala, Z. Amitay, B. Zhang, S. R. Leone, and R. Kosloff, *Phys. Rev. A* **66**, 062316 (2002).
185. D. R. Glenn, D. A. Lidar, and V. A. Apkarian, *Mol. Phys.* **104**, 1249 (2006).
186. B. P. Lanyon, J. D. Whitfield, G. G. Gillett, M. E. Goggin, M. P. Almeida, I. Kassal, J. D. Biamonte, et al., *Nat. Chem.* **2**, 106 (2010).
187. A. Aspuru-Guzik and P. Walther, *Nat. Phys.* **8**(4), 285–291 (2012).
188. D. Akoury, et al., *Science* **318**, 949 (2007).
189. J. P. Dowling and G. J. Milburn, *Philos. Trans. R. Soc. Lon. A* **361**, 1655–1674 (2003).